



Phenology, fluxes and their drivers in major Indian agroecosystems: A modeling study using the Community Land Model (CLM5)

K. Narender Reddy¹, and Somnath Baidya Roy¹

¹Centre for Atmospheric Sciences, Indian Institute of Technology Delhi, New Delhi, Delhi, India, 110016.

5 *Correspondence to:* K Narender Reddy (knreddy@cas.iitd.ac.in)

Abstract. Agroecosystems are the largest land use category covering more than half of the land surface in India, yet the understanding of spatio-temporal variability of the terrestrial fluxes over these ecosystems is limited. Previous studies are mostly at site-scale relying on eddy covariance observations that fail to capture the spatial variations across diverse climatic regions of India. The only regional scale study, Reddy et al. (2023), limits to wheat crop and lacks the robust model calibration, leading to higher uncertainties in simulated crop physiology and carbon uptake across diverse climatic regions. This study is the first to comprehensively investigate long-term trends (1970–2014) in crop physiological parameters and terrestrial fluxes across major croplands of India. This study uses a robustly calibrated Community Land Model version 5 (CLM5) to conduct numerical experiments for understanding the influence of natural and management factors on crop physiology and terrestrial fluxes. CLM5 simulations show Pearson's correlation coefficients exceeding 0.6 for regional carbon fluxes and 0.95 for regional yield estimates. The results show that crop physiology parameters have increased more than twofold since the 1970s, with crop carbon uptake by agroecosystems doubling, while respiratory losses decreased due to improved nitrogen fertilization. The largest impact is due to nitrogen fertilizer usage and nitrogen related processes which contributed to more than 50% of the observed trend in crop physiology parameters and carbon uptake in both rice and wheat. Followed by irrigation application and increasing atmospheric carbon concentration. The results further reveal that CLM5 performs particularly well in estimating carbon fluxes during the cold, dry rabi season, and simulates water and energy fluxes more accurately during the warm, wet kharif season. The results highlight the need to investigate the stomatal activity for crops in CLM5 and understand the reason for comparatively poor simulation of carbon fluxes in the kharif season and water and energy fluxes in the rabi season. This is the first study to address both the spatial and temporal variations in agroecosystem physiology and fluxes in India using a robustly calibrated and evaluated land model. Given the scarcity of studies on terrestrial fluxes in tropical agroecosystems, this work demonstrates the importance of using limited site-scale data to improve regional-scale models and enhance our understanding of tropical agroecosystems.

1 Introduction

The exchange of carbon, water, and energy between the ecosystem and atmosphere are the fundamental biophysical and biogeochemical processes within the biosphere. The influence of these exchanges on climate and environmental changes spans from regional to global scales (Bonan and Doney, 2018; Migliavacca et al., 2021). In recent decades, significant changes have



been observed in the carbon and water cycles, as well as the energy balance of terrestrial ecosystems, driven by climate change and human activities (Zhu et al., 2016; Piao et al., 2020; Konecky et al., 2023; Niu et al., 2023). Examining and understanding the changes in the carbon, water, and energy cycles, the primary factors and prevailing mechanisms driving the changes is essential for planning adaptive measures (Yu et al., 2024).

35 Agroecosystems constitute a substantial portion of the terrestrial ecosystem and have a considerable influence on the land-atmosphere interactions (Liu et al., 2016; Lokupitiya et al., 2016; Ingwersen et al., 2018). Agroecosystems are influenced by natural factors, including temperature, radiation, precipitation, and atmospheric CO₂, as well as human management factors like irrigation, nitrogen fertilization, tillage, and residual management (Chenu et al., 2017). Any change in natural and management drivers exerts varied impacts on agroecosystems (Gahlot et al., 2020; Lombardozzi et al., 2020; Reddy et al.,
40 2023). In India, almost 56% of the land is comprised of farms (Zanaga et al., 2021), 80% of which is for wheat and rice. These two crops play a crucial role in supplying vital food to the expanding population of India while also influencing terrestrial carbon, water, and energy fluxes throughout their growing season. The combined growing season of the two crops spans approximately 240-280 days, with peak growth occurring for nearly 4-6 months annually. Terrestrial fluxes from rice and wheat croplands dominate regional land-atmosphere interaction processes. Hence, it is important to understand the dynamics
45 of crop phenology and fluxes and their drivers in these agroecosystems.

In the past twenty years, there has been extensive investigation into terrestrial fluxes in agroecosystems, utilizing station-level eddy covariance techniques globally. Investigations into the rice ecosystem fluxes were conducted in Japan (Saito et al., 2005), the Philippines (Alberto et al., 2009), Bangladesh (Hossen et al., 2011), and China (Chen et al., 2015). The wheat ecosystems were examined in Germany (Schmidt et al., 2012), China (Chen et al., 2015), and the USA (Wagle et al., 2021). The
50 investigations into wheat ecosystems in Germany, China and United States typically have a significantly longer growing period compared to the wheat growing seasons in India, owing to the vernalization period experienced in mid-latitude regions. Therefore, the estimates of terrestrial fluxes in mid latitude countries are not representative of a tropical country like India. A few site-scale studies have examined the terrestrial fluxes within Indian agroecosystems as well (Patel et al., 2011; Bhattacharya et al., 2013; Kumar et al., 2021; Patel et al., 2021). These studies are performed at one site and typically examine
55 a brief timeframe, generally 1-3 growing seasons, which fail to adequately represent the diverse climatic growing regions of India. For example, the study sites in Patel et al. (2011, 2021) and Kumar et al. (2021) are in the northern part of India, which has colder temperatures and is well irrigated. They are not representative of all wheat-growing regions of India, most of which experience warm temperatures and water stress due to low water availability (Gahlot et al., 2020).

Our study seeks to tackle the following gaps: (1) the lack of regional estimates of crop phenology, productivity, and terrestrial
60 fluxes over the agroecosystems of India; (2) lack of estimates of long-term trends and changes in crop phenology, productivity, and terrestrial fluxes; and (3) lack of understanding of the drivers responsible for the observed trends. The study period spans almost 50 years (1970 to 2014), allowing for an examination of the long-term changes in crop phenology, productivity, and terrestrial fluxes influenced by climate change and human-induced factors, as well as an estimation of spatial variation.



Land surface models are an excellent tool for investigating terrestrial fluxes and how various drivers will impact the fluxes. These models have come a long way, from their initial versions of simple land representation for providing boundary conditions to the atmospheric models to very complex models currently, with accurate representations of the land units present on the surface and their complex interactions and competition for resources (Fisher and Koven, 2020). The International Land Model Benchmarking (ILAMB), which rates the performance of the land surface models, reported that CLM has good complexity in its representation of the land surface and simulates their interactions much better than any other land model (Collier et al., 2018). The latest version of the CLM, CLM5, is selected for investigating the Indian agroecosystems. Over the past decades, CLM has been widely used to improve our understanding of terrestrial energy, water, and carbon cycle dynamics and their interactions (Green et al., 2019; Koven et al., 2017; Lei et al., 2014; Li et al., 2015; McGuire et al., 2018), the impact of land use and land cover change on climate, carbon, water, and extremes (Lawrence and Chase, 2010; Lawrence et al., 2018b; Mahowald et al., 2016). Gahlot et al. (2020) and Reddy et al. (2023) investigated the impact of natural and management drivers on crop phenology and carbon fluxes in spring wheat agroecosystems, respectively, using the Integrated Science Assessment Model (ISAM) land surface model at a regional scale. The major limitation of these studies is using only one site for calibration. Additional limitation is simulating only wheat rather than all vegetation types over the Indian region. Wheat is mostly harvested in northern part of India during rabi season and constitutes to 30 Mha, while rice is harvested across India in the kharif (39 Mha) and rabi (5 Mha) seasons (ASG-2023, 2024). Therefore, the current study expands on the Indian harvested land area by investigating wheat and rice crops, which constitute nearly 80% of the agricultural land of India. Furthermore, this study uses CLM5 model that is calibrated against multiple site scale data.

CLM5 has deficiencies in simulating rice and wheat growing seasons in India. Reddy et al. (2025) utilized data collected at 15 sites in India with different climatic conditions to improve the model. The current study employs the improved CLM5 model to simulate crop phenology, fluxes and examine the influence of natural and management drivers in rice and wheat croplands of India. The study accounts for changing climate and carbon dioxide (CO₂) concentration in the atmosphere as the natural drivers and fertilization and irrigation as the human management factors. The specific objectives of the study are to (1) evaluate the CLM5 simulation of crop phenology and terrestrial fluxes against the site scale and regional scale data; (2) investigate the temporal and spatial trends of crop phenology and fluxes; and finally, (3) understand the impact of natural and management drivers on the observed trends.

Given the scarcity of studies on terrestrial fluxes in tropical agroecosystems, this work not only underscores the importance of leveraging limited site-scale data to refine regional-scale models but also highlights the potential for improving predictions of agricultural responses to climate change. By enhancing our understanding of the spatial and temporal dynamics of crop productivity, carbon, and water fluxes in a highly diverse and climatically sensitive region like India, this study provides valuable insights for future food security planning and sustainable land management. The approach demonstrated in Reddy et al. (2025) and in this study can serve as a blueprint for extending such analyses to other tropical and subtropical regions, where data limitations and complex agroecosystem interactions are observed. Ultimately, this research contributes to global efforts in predicting agricultural resilience, optimizing resource use, and mitigating the impacts of climate change on agroecosystems.



2 Methodology

2.1 Community Land Model Version 5 (CLM5)

- 100 CLM5 is the latest land component version in the Community Earth System Model (CESM) (Lawrence et al., 2018, 2019). The biogeochemistry mode of CLM5 (CLM5-BGC) is widely used to estimate the water, energy, and carbon fluxes in various climatic zones (Cheng et al., 2021; Denager et al., 2023; Song et al., 2020; Seo and Kim, 2023). The biogeochemistry and crop module of CLM5 (BGC-Crop) is modified in various studies to meet regional constraints, and the resulting impact on various fluxes is analyzed (Boas et al., 2021; Boas et al., 2023; Raczka et al., 2021; Yin et al., 2023). The CLM5 crop module includes
- 105 new crop functional types, updated fertilization rates and irrigation triggers, a transient crop management option, and some adjustments to phenological parameters (Lombardozi et al., 2020; Cheng et al., 2021).
- Reddy et al. (2025) has shown that the CLM5 model has significant deficiencies in simulating Indian crops. The growing seasons of wheat and rice were off by 4-6 months. This has caused the crops to grow in seasons which is not observed in India and was one of the reasons for the observed biases in simulated LAI, yield, and terrestrial fluxes. The other major reason for
- 110 the biases in CLM5 simulation was the use of parameters that are calibrated for mid-latitude regions. Reddy et al. (2025) addressed these issues by calibrating the CLM5 model for the Indian region using a novel crop dataset put together from studies conducted at Indian agricultural colleges and institutions (Further information on the novel crop data in Section 2.3.1). The improvements in the CLM5 model were made in two phases. First, the crop planting window was changed and crop growth parameters that impact the planting, phenological stages, and yield were calibrated. Second, because the crops in India
- 115 experience a varying climatic condition from south of the country to the north, a latitudinal variation in base temperature, which is part of GDD calculation (Eq. 1), was calibrated for wheat crop and was introduced for rice crop which was missing in the default CLM5 model. The modifications to the model have resulted in improvements in the site scale model simulated wheat LAI bias from 0.81 to 0.43 and Pearson correlation from -0.45 to 0.30. The overall bias in simulating crop growth has improved from 0.51 to 0.24 and 0.48 to 0.25, respectively, for wheat and rice crops (Reddy et al., 2025).
- 120 The present study uses the CLM5 model from Reddy et al. (2025) to examine the trends in agricultural activities and the impact of various drivers on terrestrial fluxes. The CLM5_Mod2 version from Reddy et al. (2025) was the best in simulating crop phenology variation across sites and regional terrestrial fluxes during the crop-growing seasons. Therefore, the CLM5_Mod2 version of the model is used in this study.

2.1.1 Carbon fluxes in crops

- 125 CO₂ is taken up by the crops through photosynthesis, and a part of it is used to meet the maintenance and growth needs, and the remaining is converted to dry matter and distributed to various crop parts. Gross Primary Production (GPP) is the total acclimated CO₂. Net Primary Production (NPP) is the difference between GPP and autotrophic respiration. Respiration in CLM5 is divided into two parts: maintenance respiration and growth respiration. Maintenance respiration is defined as the carbon cost to support the metabolic activity of existing live tissue. In contrast, growth respiration is the additional carbon cost



- 130 for synthesizing new growth. Maintenance respiration costs are directly proportional to the nitrogen content per unit area in plant parts and inversely proportional to the mean 10-day air temperature (Text S1). The CO₂ assimilated from the atmosphere (GPP) by C3 crops in CLM5 is mainly limited by Rubisco availability, photosynthetically active radiation, and Triose phosphate utilization (product availability) (Text S1). The assimilation is also limited by 10-day mean air temperature and leaf nitrogen availability.
- 135 The Total Ecosystem Respiration (TER) is the sum of Autotrophic Respiration (Ra) and Heterotrophic Respiration (Rh). Ra is the sum of maintenance, growth, and dark respiration (Text S1). In CLM5, Ra is specific to plant functional type, while Rh is specific to the land unit. Net Ecosystem Productivity (NEP) is the difference between GPP and TER.

2.1.2 Crop phenological stages

- The crops are represented mechanistically in a land surface model. The crop growth, assimilation of dry matter, and its distribution to different parts of the crop are controlled using the phenological stages. In the early stages of crop growth, more dry matter is directed toward roots and leaves to support the crop growth. During the later stages more dry matter is directed towards the reproductive parts so as to facilitate the new crop growth. The crop module simulates the phenological stages using the thermal units (GDD- Growing Degree Days), and it helps the model to direct the assimilated dry matter to the essential parts during various stages of crop growth.
- 140 CLM5 uses the AgroIBIS crop phenology algorithm (Badger and Dirmeyer, 2015; Levis et al., 2016), consisting of three distinct phases. Phase 1 starts at planting and ends with leaf emergence, phase 2 continues from leaf emergence to the beginning of grain fill, and phase 3 starts from the beginning of grain fill and ends with physiological maturity and harvest. The GDD required for maturity are input parameters to the model and are often derived from observations. GDD for maturity in rice is 2100 °C-days and 1700 °C-days for wheat. Different phenological stages of a crop, such as emergence, grain fill, and harvest, are reached when a fixed ratio of GDD maturity is reached. For example, after sowing of the crop, emergence is reached when daily accumulated GDD reaches 3% of GDD maturity, and the grain fill stage is reached when daily accumulated GDD reaches 60% of GDD maturity. Daily accumulated GDD is calculated using **Eq. 1**
- 150

$$GDD_i = GDD_{i-1} + T_{2m} - T_{base} \quad \text{Eq. 1}$$

- where GDD_i is the daily GDD accumulated over i days since sowing, GDD_{i-1} is the daily GDD accumulated over $i-1$ days since sowing, T_{2m} is the 2-meter temperature, and T_{base} is the base temperature, defined for each crop type in CLM5. Daily accumulated GDD defines the phenological stages of the crop.
- 155

2.1.3 Surface Energy and Water Fluxes

- The surface sensible and latent heat fluxes in CLM5 are defined by the Monin-Obukhov similarity theory (Lawrence et al., 2019), which relates the turbulent fluxes to the differences in mean temperature and humidity, respectively (Wang and Dickinson, 2012). The surface heat and water fluxes are defined as the contributions from the bare ground and the vegetation while neglecting the impact of air within the canopy. The sensible heat flux over vegetated land units is the sum of heat flux
- 160



from the ground surface and heat flux from vegetation. Similarly, the latent heat flux over vegetated land units is the sum of water vapor fluxes from the ground surface and vegetation. The water vapor flux from vegetation is the sum of water vapor flux from wetted leaf and stem area, i.e., water evaporation intercepted by the canopy and transpiration from dry leaf surfaces (Lawrence et al., 2018). This study considered the total heat and water vapor fluxes from the land units over wheat and rice-growing regions of India.

2.1.4 Nitrogen Fertilization and Irrigation

CLM simulates fertilization by adding nitrogen directly into the mineral nitrogen reservoir of soil to satisfy crop nitrogen requirements. A dedicated agricultural land unit in CLM guarantees that natural vegetation will not utilize the fertilizer supplied to crops. In CLM5, fertilizer application is determined by crop functional types and varies spatially each year according to the LUMIP land use and land cover change time series (Lawrence et al. 2016). Fertilizer application commences during the leaf emerging phase of crop growth (phase 2) and persists for 20 days, mitigating significant nitrogen losses due to leaching and denitrification in the early stages of crop development (Lawrence et al. 2019).

The CLM irrigates the cropland areas that are equipped for irrigation. The implementation of irrigation adapts dynamically to the soil moisture conditions modeled by CLM. The irrigation algorithm is based on the work of Ozdogan et al. (2010). Upon enabling irrigation, the crop fields inside each grid cell are partitioned into irrigated and rainfed fractions based on a dataset identifying regions equipped for irrigation (Portmann et al. 2010). Irrigated and rainfed crops reside on distinct soil columns, ensuring that irrigation is exclusively simulated to the soil beneath the irrigated crops. In irrigated agricultural fields, an assessment is conducted daily to determine the necessity of irrigation for that day. This verification occurs during the initial time step following 6 AM local time. Irrigation is necessary when the crop leaf area exceeds zero and the available soil water falls below a designated threshold (Lawrence et al., 2019).

2.2 Details of experiments

In this study, the model simulations are land-only simulations with active biogeochemistry and active crops at 0.5° resolution using the Global Soil Wetness Programme Phase 3 (GSWP3) atmospheric forcing data. CLM5 is spun up for 200 years in an accelerated mode and 400 years in normal mode to achieve equilibrium conditions. The regional domain used in the study is 0° N to 40° N and 60° E to 100° E. This simulation is the Control run and is referred to as CTRL throughout the manuscript. We conducted four additional experiments to evaluate the impact of various drivers on the observed trends: S_{Clim} , S_{CO_2} , S_{NFert} , and S_{Irrig} (Table 1). S_{Clim} is simulated using the 1901-1920 GSWP3 data cycled over for 50 years (from 1965 to 2014). S_{CO_2} is simulated using the pre-industrial CO_2 levels in the atmosphere while keeping all other drivers similar to the CTRL simulation. S_{NFert} is simulated by turning off the nitrogen fertilization for crops. Similarly, S_{Irrig} is simulated by turning off irrigation for crops.

All CLM5 simulations are run from 1965 to 2014, and the data from 1970-2014 is used in the analysis. The initial five years of the CLM5 simulations are discarded so as to minimize the initial noise in crop growth.



Table 1: Description of CLM5 simulations conducted in this study and the constraints used to extract the impact of individual drivers

Numerical Experiment	Climate	[CO ₂]	Nitrogen Fertilization	Irrigation
CTRL	HIST-GSWP3 1-hourly atmospheric data	Diagnostic CO ₂	Yes	Yes
S _{Clim}	1901-1920 GSWP3 data	Diagnostic CO ₂	Yes	Yes
S _{CO2}	HIST-GSWP3 1-hourly atmospheric data	Pre-industrial CO₂ (284.7 ppm)	Yes	Yes
S _{NFert}	HIST-GSWP3 1-hourly atmospheric data	Diagnostic CO ₂	No	Yes
S _{Irrig}	HIST-GSWP3 1-hourly atmospheric data	Diagnostic CO ₂	Yes	No

195

2.3 Evaluation of CLM5

2.3.1 Crop physiological parameters

The crop physiological parameters simulated in the CTRL simulation are evaluated using the site scale data from 1970 to 2014 (Varma et al., 2024). The site scale observation data was generated by digitizing the thesis results of students pursuing a Master or PhD degree in various agricultural colleges across India (Varma et al., 2024; Reddy et al., 2025). A part of the crop data from 2000 to 2014 was used to calibrate and validate the CLM5 model in Reddy et al. (2025). The data has a variety of experiments ranging from varying nitrogen fertilization, planting dates, irrigation, weed management, and others. Only the control experiment data at the sites is used for evaluating CLM5 in this study. If any dataset in Varma et al. (2024) has multiple sowing dates, the sowing date mentioned as normal sowing is used for CLM5 model evaluation.

The crop physiological parameters considered for evaluation are LAI (m²/m²), grain yield (GY) (t/ha), and total dry matter (DM) (t/ha). The evaluation metrics reported here are Mean Absolute Bias (MAB), Pearson’s correlation (*r*), and Root Mean Square Error (RMSE).



$$MAB = \frac{\sum |CLM_{var} - Obs_{var}|}{\sum (Obs_{var})} \quad \text{Eq. 2}$$

$$RMSE = \sqrt{\frac{\sum (CLM_{var} - Obs_{var})^2}{N}} \quad \text{Eq. 3}$$

$$r = \frac{\sum (CLM_{var} - \overline{CLM_{var}})(Obs_{var} - \overline{Obs_{var}})}{\sqrt{\sum (CLM_{var} - \overline{CLM_{var}})^2 \sum (Obs_{var} - \overline{Obs_{var}})^2}} \quad \text{Eq. 4}$$

where var is the crop phenology variable, CLM_{var} and Obs_{var} are the simulated and observed variable values, $\overline{CLM_{var}}$ and $\overline{Obs_{var}}$ are the respective mean values.

CLM5 yield is also compared against the FAO annual data for wheat and rice from 1970-2014. The CLM5 yield is the CTRL simulation spatial average of wheat and rice yield across the wheat and rice growing regions. The FAOSTAT database (FAO, 2022a) provides country-level data on area harvested and production for every year starting in 1961. The country-scale annual yield is derived by dividing production by the area harvested for the wheat and rice crops.

2.3.2 Terrestrial fluxes

The accurate simulation of carbon fluxes in various ecosystems by CLM5 is essential for two reasons. 1) The accurate simulation of carbon fluxes in agroecosystems during the growing season will result in an accurate simulation of crop growth, and 2) the accurate simulation of carbon fluxes in all ecosystems will provide us confidence in the carbon uptake estimates by various ecosystems in a changing climate. To validate the carbon fluxes and other water and energy fluxes in Indian agroecosystems, we have compared the fluxes with both available site scale data and regional scale reanalysis data.

2.3.2.1 Site scale carbon fluxes

Carbon flux studies in Indian agroecosystems are limited, and the data they produce is not available publicly. Patel et al. (2011), Patel et al. (2021), and Bhattacharya et al. (2013) investigated the terrestrial fluxes in Indian agroecosystems, but the raw data is not provided. Hence, the data is extracted from figures in the manuscripts using plotdigitizer software (PlotDigitizer, 2025). Patel et al. (2011) investigated the carbon fluxes in a wheat field in Meerut (29°05' N, 77°41' E) during the 2009-10 growing season (December to April) and reported the fluxes as diurnal cycles during various phenological stages (Figure 2 in Patel et al. (2011)). The monthly mean values are generated from the diurnal cycles. Bhattacharya et al. (2013) investigated the carbon fluxes in rice fields at Cuttack (20°27' N, 85°56' E) in the kharif season in 2010 and reported the fluxes as diurnal cycles during various phenological stages (Figure 1 in Bhattacharya et al. (2013)). The monthly mean is generated from the diurnal cycles. Reddy et al. (2023) used the carbon fluxes measured in a wheat field at IARI, New Delhi (28°40' N, 77°12' E), during the growing season of 2013-14 to validate the ISAM carbon fluxes. The site scale wheat carbon fluxes data at IARI is generated by Kumar et al. (2021) and the fluxes are reported as monthly means.

For site-scale evaluation and analysis, CLM5 simulated crop carbon flux estimates from the grid cell corresponding to the latitude and longitude of the site are extracted. The site scale wheat flux data (GPP, TER, and NEP) from Reddy et al. (2023) is compared against the wheat monthly mean carbon fluxes of CTRL simulation. The site scale rice flux data (GPP) from Bhattacharya et al. (2013) and wheat flux data (NEP) from Patel et al. (2011) is compared against the respective crop carbon



fluxes from CTRL simulation. Comparing the CLM5 CTRL carbon fluxes of major Indian agroecosystems against the
240 corresponding fluxes in observations will provide the uncertainty in CLM5 simulations and help us better understand the trends
and impacts of multiple drivers.

2.3.2.2 Regional scale carbon, water, and energy fluxes

We used the FLUXCOM reanalysis data to evaluate the CTRL simulation terrestrial fluxes at the regional scale. FLUXCOM
data is generated using machine learning to merge the flux measurements in eddy covariance towers with remote sensing and
245 meteorological data and estimate surface fluxes (Jung et al., 2019). We used the monthly 0.5° resolution RS_METEO version
of the FLUXCOM data for comparison against the CLM5 simulations. We compared the monthly spatial average of terrestrial
fluxes against those from CLM5 simulations. The energy and water fluxes are available from 1950 to 2014, while the carbon
fluxes are available from 2001 to 2014 in the FLUXCOM data. Hence, energy and water fluxes simulated by CLM5 from 1970
to 2014 are evaluated against the FLUXCOM data, while CLM5 simulated carbon fluxes data is evaluated for the period 2001
250 to 2014.

2.4 Impact of drivers on crop phenology and terrestrial fluxes

Numerical experiments (Table 1) are conducted to understand the impact of individual drivers on terrestrial fluxes and crop
phenology. The Mann-Kendall test (Hussain and Mahmud, 2019) is used to estimate if a trend exists in the CTRL run, and the
Theil-Sen slope is reported. The significance of the slope is tested using the Student's two-tailed test at a significance level of
255 $p < .05$. The trend in the impact of individual drivers is analyzed by finding the slope of CTRL- S_{driver} . If the slope is high and
significant at $p < .05$, that particular driver has a significant impact on the agroecosystem. If the slope is near zero and p value
is higher than the threshold (0.05), then the driver has no significant impact on the agroecosystem.

3 Results

3.1 Evaluation of crop physiological parameters and terrestrial fluxes

260 3.1.1 Crop parameters

This study uses the best performing CLM5 model in Reddy et al. (2025) for estimating the Indian crop simulation. The Indian
crop physiology bias against the site scale observations by the default CLM5 model was very high compared to that of the
improved CLM5 model (Reddy et al., 2025). For example, the bias in the LAI simulation was 0.81 and 0.66 for wheat and rice
in the default model. The bias in LAI reduced in the improved model to 0.43 and 0.34 for wheat and rice (Reddy et al., 2025).
265 The largest improvement in crop simulation was observed in wheat growing season length, RMSE improved from 63 days in
the default case to 15 days in CLM5_Mod2 (Reddy et al., 2025). The site scale observation data from 2000 to 2014 was used
for comparing the crop physiology simulation by various versions of the CLM5 model in Reddy et al. (2025). In this study,
the observation data from 1970 to 2014 is used to validate the best performing model from Reddy et al. (2025).

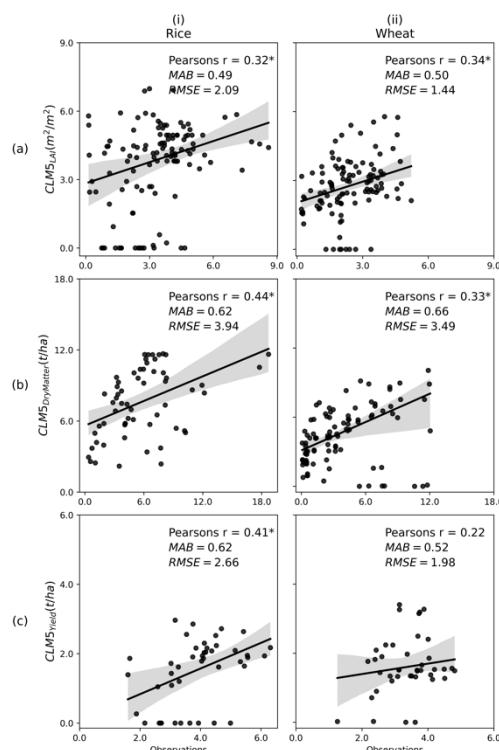


Figure 1: Scatterplot comparing site-scale observed and CLM5 simulated (a) LAI, (b) Dry Matter, and (c) Yield of (i) rice and (ii) wheat crops for 1970-2014 period. The * indicates that the correlation is statistically significant at $p < 0.05$. The black line is the best fit between the observed and simulated values, and the grey-shaded region is the 95% Confidence Interval (CI).

Figure 1 compares the crop physiological parameters simulated by CLM5 (CTRL experiment) against that of the observations from 1970-2014. The black line shows the best fit between the observations and the simulations, and the grey-shaded region shows the 95% confidence interval. Comparing the CLM5 simulated crop physiological parameters in the CTRL run against those from observations, rice simulated in the CTRL experiment is performing reasonably well, with r -values of 0.32, 0.44, and 0.41 for LAI, total dry matter, and yield, respectively, significant at $p < 0.05$. Similarly, wheat simulated in the CTRL experiment is performing well with r -values of 0.34, 0.33, and 0.22 for LAI, total dry matter, and yield respectively. The bias in crop parameters is 0.5-0.7 in Figure 1. The bias in rice and wheat simulated by the default CLM5 model in Reddy et al. (2025) was in the range of 0.7-0.8.

The RMSE in yield estimates (Figure 1c) is high, with 2.66 and 1.98 t/ha, for rice and wheat, respectively. The high RMSE is due to a few sites having zero yield. CLM5 did not simulate the crop growth for a few years in the region because the grid cell had zero crop area in a particular year indicating a discrepancy between the land cover data used in CLM5 and the ground reality. Therefore, CLM5 simulated zero yield for the corresponding year and grid cell. However, when we compare the FAO mean yield over the Indian region against that of the CLM5 simulation, the trend observed in FAO data is replicated by CLM5 simulation of rice ($r=0.96$) and wheat ($r=0.96$) (Figure 2). This shows that, although there are regional discrepancies in yield



simulations for individual crops due to a number of reasons, the average crop yields at the country scale are very close to observations. The bias and RMSE are also very low for wheat and rice simulations at the country-scale.

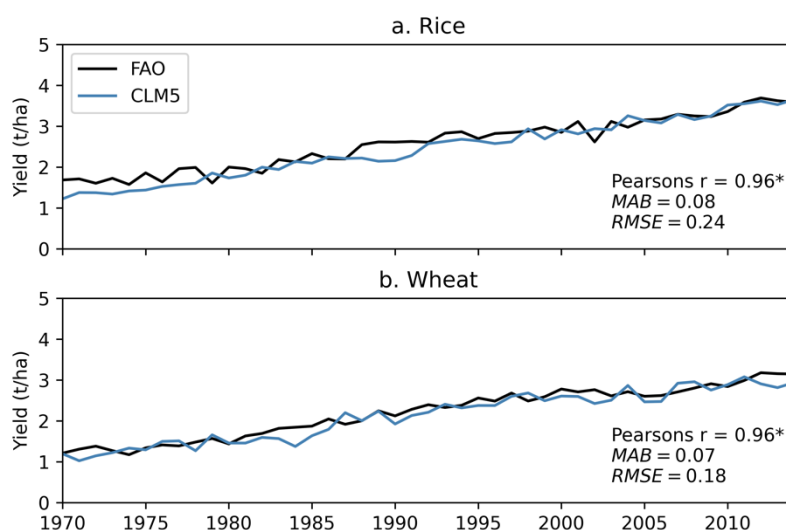


Figure 2: Comparison of yield simulated by CLM5 for major Indian crops (a) Rice and (b) Wheat against the FAO observations

3.1.2 Carbon fluxes

3.1.2.1 Site scale evaluation

The carbon fluxes simulated by CLM5 are evaluated by comparing against those from observations (Figure 3) at Cuttack (20°27' N, 85°56' E), IARI, New Delhi (28°40' N, 77°12' E), and Meerut (29°05' N, 77°41' E). Figures 3a, 3b and 3c compare the GPP, TER, and NEP, respectively, measured in a wheat field at IARI, New Delhi, during the rabi season of 2013-14 against the CLM5 simulated monthly mean carbon fluxes. The CLM5 simulations overestimate the fluxes during the early months and are close to observation estimates in the reproductive and maturity months. In CLM5, GPP is specific to the crop, while TER is the sum of crop-specific term (R_a) and R_h , which is representative of the cropland unit (explained in section 2.1.1). Due to this discrepancy in flux estimates in CLM5, especially TER, and NEP, we observe high bias when we compare them against the site scale carbon estimates.

Figure 3d compares the NEP measured at Meerut during the rabi season of 2009-10 over a wheat field against that of the CLM5 simulations. Analysing the NEP simulated by CLM5 at Meerut, although an erroneous high value is simulated in March, the fluxes simulated by CLM5 are close to observations in other three months (January, February, and April). Figure 3e compares the GPP measured during the 2010 kharif season, against the CLM5 carbon fluxes. The CLM5 simulations overestimate the GPP. One reason for the low GPP at the site might be because the farmland was flooded (Liu et al., 2013), while the CLM5 does not simulate a flooded rice field. The overall monthly mean carbon fluxes simulated by CLM5 are compared against that of observations in a scatter plot in Figure 3f. The dark black line shows the linear regressed data, and



the shaded region shows the 95% confidence interval. The Pearson r value between observations and CLM5 simulations is high (0.65) and is significant at $p < .001$.

310 Site level comparison (Figure 3a-e) of fluxes shows varied results due to the following reasons: 1) the site scale data is an average of infrequent and irregular sample taken during a phenological stage while the simulated data is an average of daily means. 2) differences in the sowing dates of crops by 3-4 weeks between the site and the model, and 3) Rh is not crop specific but defined for a land type in CLM5, and that introduces uncertainties in TER and NEP estimates of CLM5. In spite of these differences, Figure 3(f) clearly demonstrates that CLM5 simulates carbon fluxes with good seasonality ($r=0.65$) and low bias

315 (0.67).

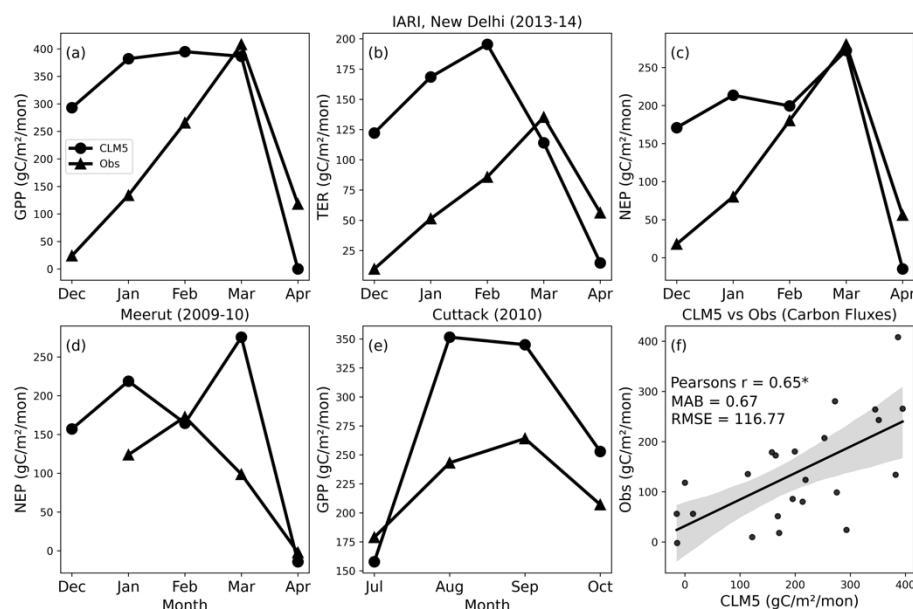


Figure 3: Comparing CLM5 carbon fluxes against observations of (a, b, and c) wheat cropland at IARI, New Delhi, from a study by Reddy et al. (2023), (d) wheat cropland at Meerut, from a study by Patel et al. (2011), (e) rice cropland at Cuttack from Bhattacharya et al. (2013), and (f) scatter plot of all monthly mean carbon flux observations against the monthly mean carbon fluxes from CLM5. The ‘*’ on Pearson r in panel (f) signifies the statistical significance at $p < .001$. The solid black line in (f) is the linear regression, and the shaded region is the 95% confidence interval.

3.1.2.1 Regional scale

Figures 4 and 5 show the regional comparison of GPP, TER, and NEP of CLM5 CTRL simulation against the FLUXCOM data over rice and wheat growing regions, respectively. While comparing the regional scale fluxes, we used only the grid cells

325 where more than 10% of the grid cell area is occupied by rice or wheat crop. This is done to reduce the noise and uncertainty at regional scale from regions with low crop area and evaluate the ability of CLM5 to simulate the carbon fluxes in regions with high crop cover. Figures 4 and 5 shows the seasonal mean carbon fluxes, i.e., for the rice crop, the mean fluxes over July

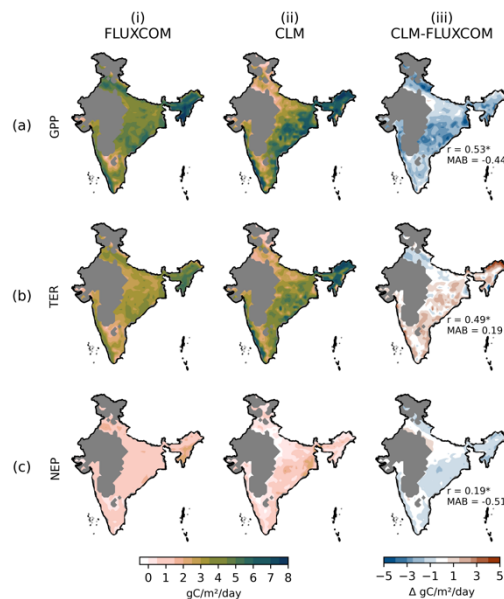


to October, and for the wheat crop, the mean fluxes over December to March, from 2000 to 2014. The spatial correlation and MAB between the CLM5 simulated carbon fluxes and the FLUXCOM data is shown in Figure 4iii.

330 Figure 4aiii shows the difference in mean seasonal GPP simulated by CLM5 over the rice-growing region and observed FLUXCOM data. CLM5 has a good spatial correlation (0.53) but is underestimating the GPP compared to the FLUXCOM data (MAB = -0.44). Figure 4biii shows that the TER simulated by CLM5 has a good spatial correlation (0.49) and a low bias (MAB=0.19). The NEP simulated by CLM5 (Figure 4ciii) has spatial variation, but the FLUXCOM data does not, and therefore, the NEP simulated by CLM5 has low spatial correlation (0.19) and high bias (-0.51) with the FLUXCOM data. All
335 spatial correlations calculated here are significant at $p < .01$ tested using a two-tailed test.

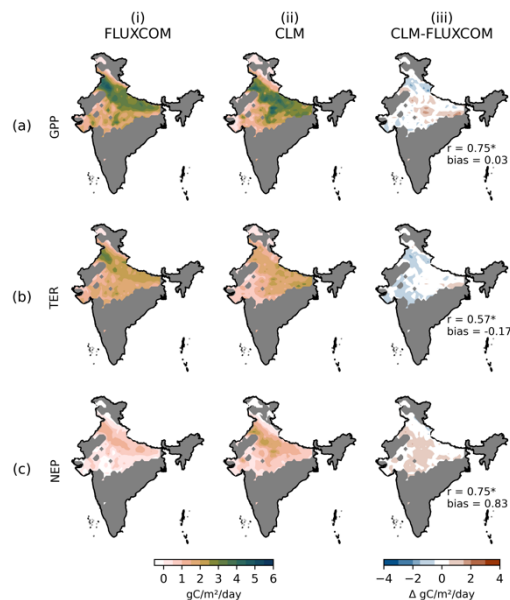
Figure 5 shows the mean seasonal GPP, TER, and NEP over the wheat-growing region from the CLM5 CTRL simulations against the FLUXCOM data. Figure 5aiii shows the difference in mean seasonal GPP simulated by CLM5 over the wheat-growing region and FLUXCOM data. CLM5 simulated GPP has a good spatial correlation (0.75) and a low bias (MAB = 0.03)
340 when compared against the FLUXCOM data. Figure 5biii shows that the TER simulated by CLM5 has a high spatial correlation (0.57) and a low bias (MAB=0.17). The NEP simulated by CLM5 (Figure 5ciii) has a high spatial variation (0.75) and a high bias (0.83). However, the bias in large parts of the wheat-growing regions is within the range of ± 0.5 gC/m²/day (shown in white in Figure 5ciii).

345 The regional comparison between carbon fluxes simulated by CLM5 and observations from FLUXCOM reveals that the carbon fluxes simulated during the kharif season (warm and wet conditions) exhibit a larger bias than that in the rabi season (cold and dry conditions). The cause of this behavior is not examined, but it is an important observation. The variation in seasonal carbon fluxes in CLM5 in different seasons might be caused by the changes in stomatal conductance at elevated temperatures and high vapor pressure deficit. GPP is calculated after accounting for respiration (Rd in supplement material: Text S1), and at high
350 temperatures and vapour pressure deficit during the warm seasons, we observe higher TER simulated by CLM5 and eventually reducing the GPP. The lower GPP and higher TER simulated by CLM5 for rice crops might also be caused due to the absence of flooded rice growth in CLM5 while most of the rice growth is in flooded conditions, especially in central India and the southern regions. And these are the regions in Figure 4 where we observe a high bias.



355

Figure 4: Spatial plots of (a) GPP, (b) TER, and (c) NEP from (i) FLUXCOM, (ii) CLM5 over the Indian region, and (iii) the difference between the CLM5 and FLUXCOM data. All plots are for the rice-growing regions (grid cells with more than 10% of land area covered by rice crop) and the mean of the data growing season (July to October). The “*” over the r value shows a significant correlation at $p < 0.01$.



360

Figure 5: Spatial plots of (a) GPP, (b) TER, and (c) NEP from (i) FLUXCOM, (ii) CLM5 over the Indian region, and (iii) the difference between the CLM5 and FLUXCOM data. All plots are for the wheat-growing regions (grid cells with more than 10% of land area covered by wheat crop) and the mean of the growing season (December to March). The “*” over the r value shows a significant correlation at $p < 0.01$.



3.1.3 Water and energy fluxes

Figures 6 and 7 show the latent and sensible heat over the rice and wheat growing regions. Figure 6 shows the average fluxes during the rice growing season, i.e., July to October. Figure 6a shows the (i) latent heat from FLUXCOM and (ii) the difference between the CLM5 CTRL simulation and FLUXCOM. The spatial correlation between CLM5 simulated latent heat fluxes and FLUXCOM is in Figure 6ai. The correlation is high and significant at $p < .01$ and the bias is low. However, an underestimation of latent heat fluxes in the IGP region is observed. The maximum bias is observed during the late vegetation and early reproductive periods, i.e., in August and September (Figure S1). However, considering the spatial correlation, CLM5 is simulating better in large parts ($r = 0.56$ in September and $r = 0.67$ in October). During the early reproductive stage, the crop reaches the maximum LAI and should have a high impact on the latent heat fluxes.

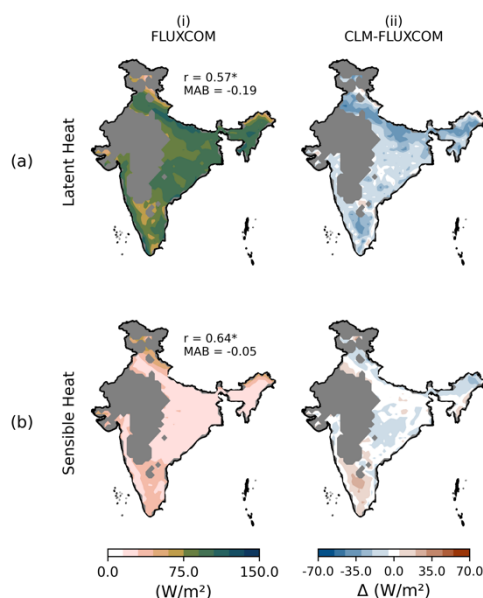


Figure 6: (a) Latent Heat, and (b) Sensible Heat from (i) FLUXCOM data, and (ii) The difference between CLM5 and FLUXCOM data, over the rice growing regions and season (July to October). All fluxes are monthly means over the period 1970 to 2014.

Figure 7 shows the average fluxes during the wheat growing season, i.e., December to March. Figure 7a show the latent heat from FLUXCOM and the difference between the CLM5 CTRL simulation and FLUXCOM. We observe a strong correlation and low bias during the rabi season. However, a consistent overestimation in the central India region is observed. During the wheat growing season, the maximum bias is observed during the early vegetation period, i.e., in December and January (Figure S2).

Figure 7b shows the sensible heat from FLUXCOM and the difference between CLM5 CTRL simulation and FLUXCOM data, respectively. Sensible heat simulated by CLM5 has a high correlation and a low bias when compared against the sensible heat estimates of the FLUXCOM data. Looking at the monthly variations during the wheat growing season (Figure S2), CLM5 simulated sensible heat is highly correlated to the FLUXCOM data and also has a low bias during all months except December.

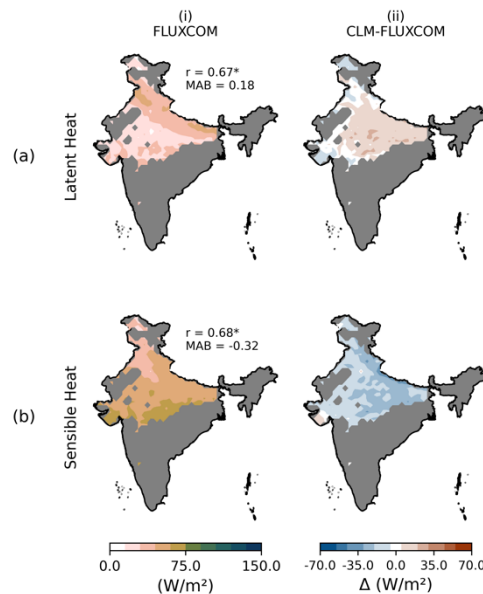


Figure 7: (a) Latent Heat, and (b) Sensible Heat from (i) FLUXCOM data, and (ii) The difference between CLM5 and FLUXCOM data, over the wheat growing region and season (December to March). All fluxes are monthly means over the period 1970 to 2014.

3.2 Trends in carbon fluxes

3.2.1 Rice

Figure 8ai shows the increasing trend in GPP from the 1970 – 2014 period. The trend in total GPP during a growing season for rice is $18 \text{ gC/m}^2/\text{year}^2$ (Figure 8ai). The annual GPP in 1970 is $1.1 \text{ kgC/m}^2/\text{year}$, while in 2014 it is $1.97 \text{ kgC/m}^2/\text{year}$. Figure 8a(ii to v) shows the impact of each of the drivers on the observed positive trend. The slopes in the figure with an asterisk are significant at $p < .05$. The slope shown in panels ‘aii’ to ‘av’ is the trend of the impact of drivers, i.e., the trend of CTRL - S_{driver} , and if the box is red in color, then the driver has a negative impact and if the box of trend is green in color, then the driver has a positive impact. The driver having a large impact on the fluxes has a higher slope in columns (ii) to (v), and the statistical significance of the impact is shown through an “*”. Climate has no significant impact on the observed annual GPP trend (Figure 8aii). CO_2 has a statistically significant positive impact on the yearly GPP trend, with a value of $11 \text{ gC/m}^2/\text{year}^2$ (Figure 8aiii). Nitrogen fertilization has a statistically significant positive impact on the annual GPP trend, with a value of $5 \text{ gC/m}^2/\text{year}^2$ (Figure 8aiv). Irrigation has a statistically significant impact with a trend of $10 \text{ gC/m}^2/\text{year}^2$ (Figure 8av). Increasing CO_2 has the largest impact on the annual GPP of rice, followed by irrigation.

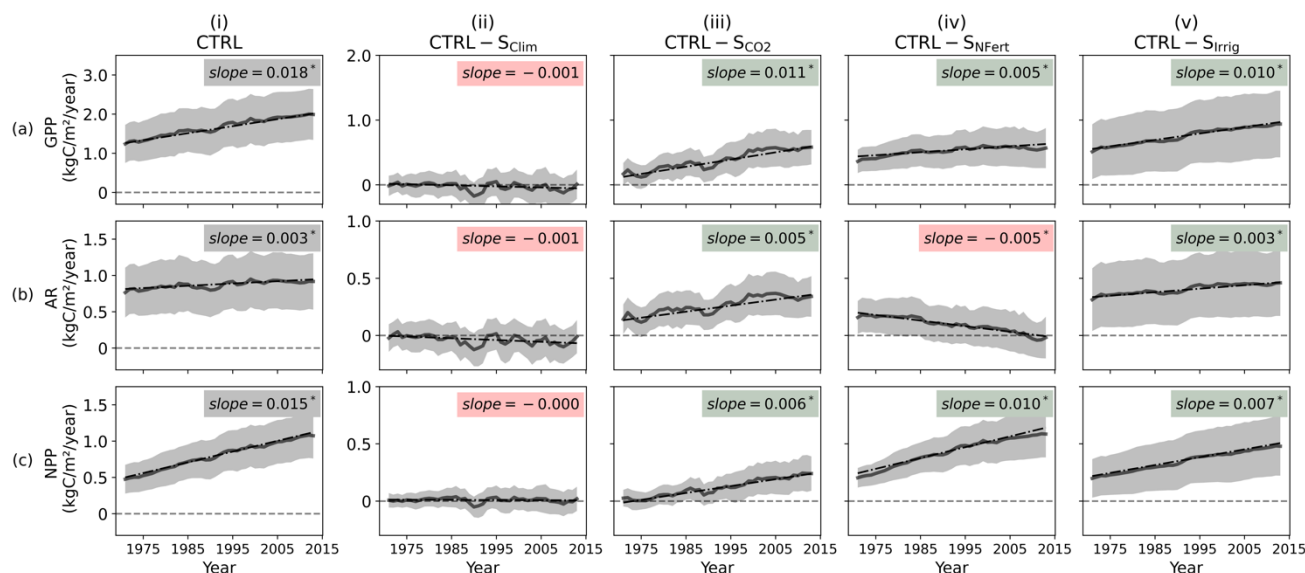


Figure 8: The moving mean (3-year period) of annual carbon fluxes in rice-growing regions (a) GPP, (b) AR, and (c) NPP in the (i) CTRL simulation from 1970 to 2014 is shown by a dark grey line. The shaded region is one standard deviation from the annual mean. The trend is calculated using Man Kendall's test. (ii) to (v) show the impact of each driver. The Sens slope of the impact is shown in the top right box of each panel, and the red box implies that the impact is negative on the crop parameter, while the green box implies that the impact is positive. Slopes marked with an asterisk mean statistically significant at $p < 0.05$.

The trend in AR for rice simulated by CLM5 from 1970 to 2014 is $3 \text{ gC/m}^2/\text{year}^2$ (Figure 8bi)). The AR simulated by CLM5 in 1970 is $0.67 \text{ kgC/m}^2/\text{year}$, while it increased to $0.90 \text{ kgC/m}^2/\text{year}$ by 2014. Figure 8bii to 8bv shows the impact of each of the drivers on the observed positive yield trend. Climate does not have a significant impact on AR in rice. CO_2 has a statistically significant positive impact on AR with a Sens slope of $5 \text{ gC/m}^2/\text{year}^2$ (Figure 8biii). Nitrogen fertilization has a statistically significant negative impact on the AR of rice, with a trend value of $-5 \text{ gC/m}^2/\text{year}^2$ from 1970 to 2014 (Figure 8biv). Irrigation has a significant positive impact on the AR of rice, with a Sens slope of $3 \text{ gC/m}^2/\text{year}^2$ during the study period (Figure 8bv). CO_2 has the most significant positive impact on AR in rice-growing regions, while nitrogen fertilization has a large negative impact on AR. This implies that rice crops tend to respire less in high nitrogen environments.

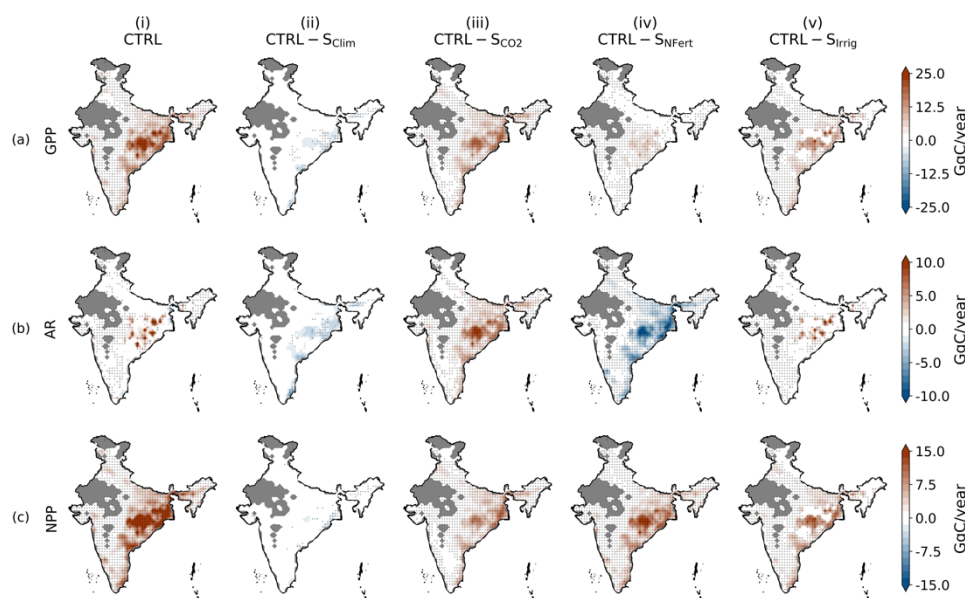


Figure 9: Spatial trend observed in carbon fluxes (a.) GPP, (b.) AR, and (c.) NPP in rice-growing regions in the (i) CTRL simulation. (ii) to (v) show the impact of each driver. Regions stippled implies the trend is statistically significant at $p < 0.05$.

The trend in NPP of rice from 1970 to 2014 is $15 \text{ gC/m}^2/\text{year}^2$ (Figure 8ci). The NPP simulated by CLM5 in 1970 for wheat is $0.43 \text{ kgC/m}^2/\text{year}$, while it increased to $1.07 \text{ kgC/m}^2/\text{year}$ by 2014. Climate has a low impact on NPP of rice that is not significant at $p < 0.05$ (Figure 8cii). CO_2 has a significant positive impact on the NPP in rice, with a trend of $6 \text{ gC/m}^2/\text{year}^2$ (Figure 8ciii). Nitrogen fertilization has a significant positive impact on the NPP of rice, with a trend of $10 \text{ gC/m}^2/\text{year}^2$ (Figure 8civ). Irrigation significantly impacts the NPP of rice, with a trend of $7 \text{ gC/m}^2/\text{year}^2$ (Figure 8cv). Nitrogen fertilization has the largest impact on the NPP during the growing season of rice, followed by irrigation and CO_2 . NPP, the carbon taken up by rice crops during their growing season, has seen the largest increase over the study period owing to the impact of nitrogen fertilization on GPP and AR. Nitrogen fertilisation has led to increasing GPP and decreasing losses through AR during the study period.

Figure 9 shows the spatial variation in the impact of various drivers over the rice-growing regions. The positive trend in GPP and NPP is significant (indicated by stippling) in all the rice-growing regions (Figure 9ai and 9ci). CO_2 , nitrogen fertilization, and irrigation impact are statistically significant over the rice growing region (Figure 9iii, 9iv, and 9v). Climate has a predominantly negative impact across the rice-growing regions but is statistically not significant (Figure 9ii). A higher increase in carbon uptake during the growing season of rice is observed in central Indian region.

3.2.2 Wheat

The trend in total GPP during a growing season for wheat is $10 \text{ gC/m}^2/\text{year}^2$ (Figure 10ai). The annual GPP in 1970 is $0.74 \text{ kgC/m}^2/\text{year}$, while in 2014 it is $1.23 \text{ kgC/m}^2/\text{year}$. Climate has a statistically significant negative impact on the observed



annual GPP trend, with a trend of $-2 \text{ gC/m}^2/\text{year}^2$ (Figure 10aii). CO_2 has a statistically significant positive impact on the annual GPP trend, with a value of $9 \text{ gC/m}^2/\text{year}^2$ (Figure 10aiii). Nitrogen fertilization has a statistically significant positive impact on the annual GPP trend, with a value of $1 \text{ gC/m}^2/\text{year}^2$ (Figure 10aiv). Irrigation has a statistically significant impact with a trend of $8 \text{ gC/m}^2/\text{year}^2$ (Figure 10av). Increasing CO_2 has the maximum impact on the annual GPP of wheat, followed by irrigation.

440 Nitrogen fertilization and climate have a low impact on GPP in wheat crops.

The trend in AR for wheat simulated by CLM5 from 1970 to 2014 is $2 \text{ gC/m}^2/\text{year}^2$ (Figure 10bi). The AR simulated by CLM5 in 1970 is $0.39 \text{ kgC/m}^2/\text{year}$, while it increased to $0.49 \text{ kgC/m}^2/\text{year}$ by 2014. Climate has a statistically significant negative impact on the AR of wheat with a value of $1 \text{ gC/m}^2/\text{year}^2$ (Figure 10bii). CO_2 has a statistically significant positive impact on AR with a Sens slope of $3 \text{ gC/m}^2/\text{year}^2$ (Figure 10biii). Nitrogen fertilization has a statistically significant negative impact on the AR of wheat, with a trend value of $-3 \text{ gC/m}^2/\text{year}^2$ from 1970 to 2014 (Figure 10biv). Irrigation has a significant positive impact on the AR of wheat, with a Sens slope of $2 \text{ gC/m}^2/\text{year}^2$ during the study period (Figure 10bv). CO_2 has the largest positive impact on AR in wheat-growing regions, while nitrogen fertilization has a large negative impact on AR. The wheat crops tend to respire more in the absence of nitrogen fertilization.

The trend in NPP of rice from 1970 to 2014 is $8 \text{ gC/m}^2/\text{year}^2$ (Figure 10ci). The NPP simulated by CLM5 in 1970 for wheat is $0.35 \text{ kgC/m}^2/\text{year}$, while it increased to $0.75 \text{ kgC/m}^2/\text{year}$ by 2014. Climate has a statistically significant negative impact on the NPP of wheat with a value of $1 \text{ gC/m}^2/\text{year}^2$ (Figure 10cii). CO_2 has a significant positive impact on the NPP in wheat, with a trend of $6 \text{ gC/m}^2/\text{year}^2$ (Figure 10ciii). Nitrogen fertilization has a significant positive impact on the NPP of wheat, with a trend of $4 \text{ gC/m}^2/\text{year}^2$ (Figure 10civ). Irrigation significantly impacts the NPP of wheat, with a trend of $6 \text{ gC/m}^2/\text{year}^2$ (Figure 10cv). CO_2 and irrigation have the largest impact on NPP during the wheat growing season, followed by nitrogen fertilization and climate. Climate has a significant negative impact on wheat crop carbon uptake which is grown in winter season (cold and dry conditions). The NPP increase in the winter wheat crop is lower than the summer rice crop.

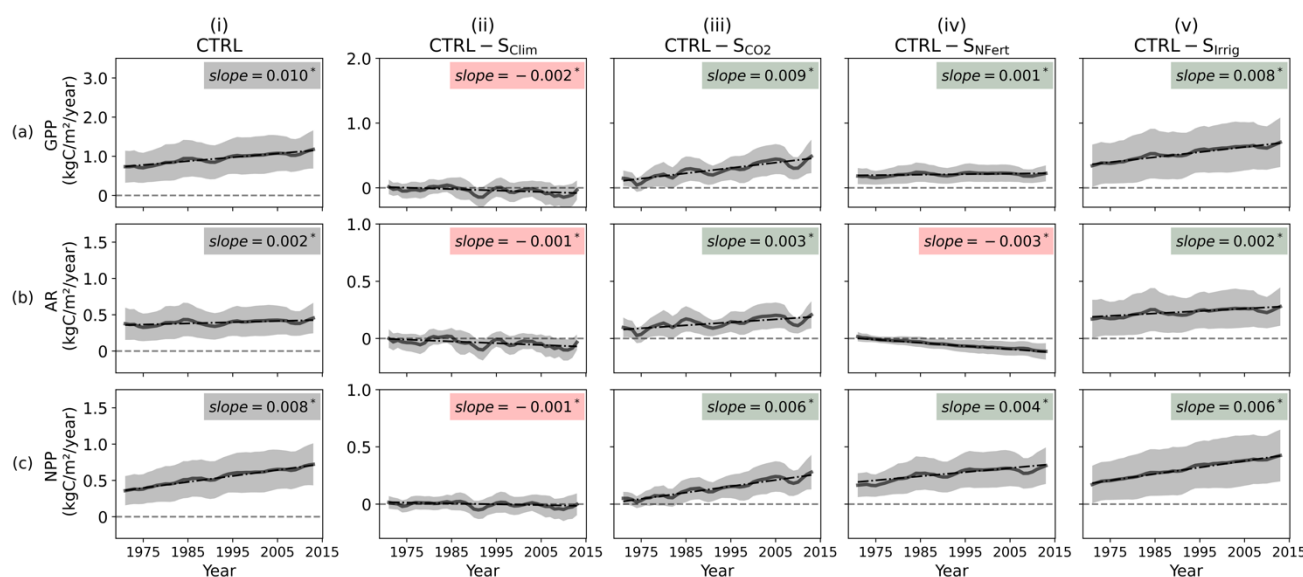




Figure 10: Similar to Figure 8, but for carbon fluxes in wheat-growing regions.

Figure 11 shows the spatial variation in the trend of carbon fluxes in the CTRL run and the impact of various drivers. GPP and NPP have positive trends across all the wheat-growing region, but higher in IGP region than others (Figure 11ai and 11ci) and are significant at $p < 0.05$. This positive trend is fuelled by higher CO_2 and irrigation in wheat growing regions (Figure 11ii and 11v). Nitrogen fertilization did not have a significant impact on GPP across all wheat growing regions, seen from scattered stippling in Figure 11aiv. However, nitrogen fertilization has significant positive impact on NPP across larger wheat region (Figure 11civ) due to significant and high negative impact on AR across all wheat growing regions (Figure 11biv).

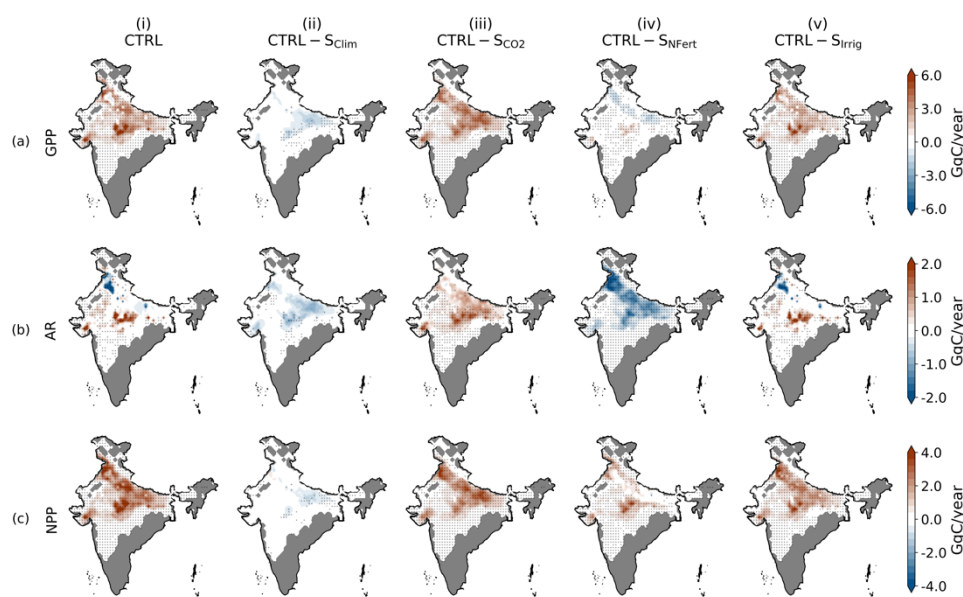


Figure 11: Spatial trend observed in carbon fluxes (a) GPP, (b) AR, and (c) NPP of wheat-growing regions in the (i) CTRL simulation. (ii) to (v) show the impact of each driver. Regions stippled implies the trend is statistically significant at $p < 0.05$.

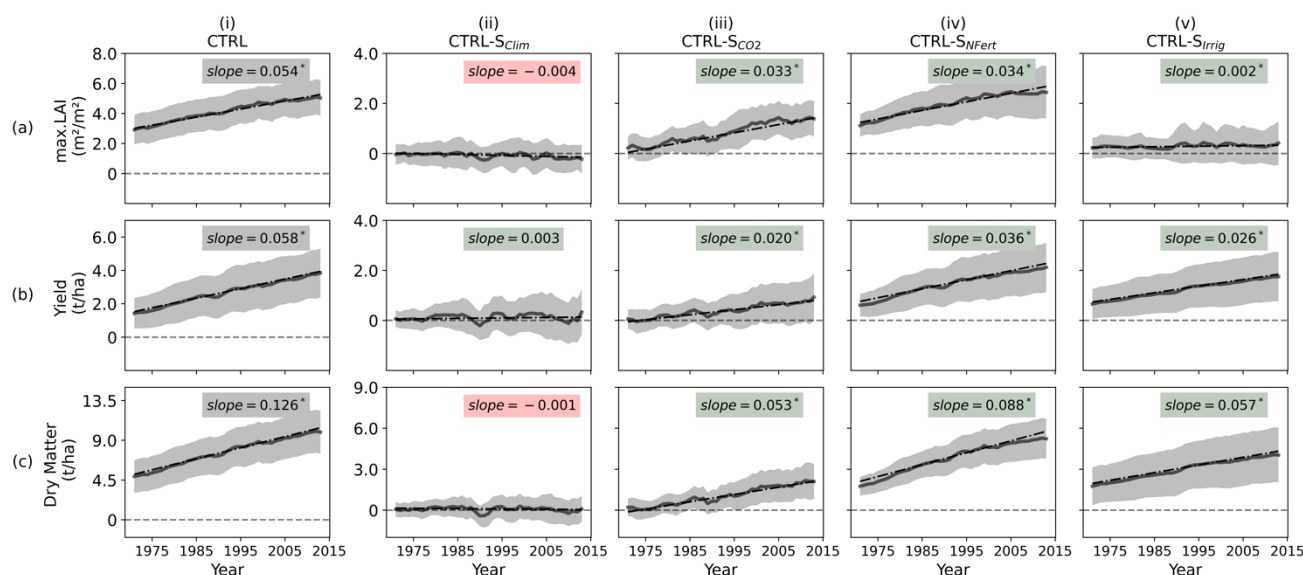
3.3 Trends in crop physiological parameters

3.3.1 Rice

The trend in maximum LAI during a growing season for rice is $0.054 \text{ m}^2/\text{m}^2/\text{year}$ (Figure 12ai). The maximum LAI in 1970 is $2.65 \text{ m}^2/\text{m}^2$, while in 2014 it is $4.88 \text{ m}^2/\text{m}^2$. Climate has a negative impact on the observed maximum LAI trend, with a trend of $-0.004 \text{ m}^2/\text{m}^2/\text{yr}$ (Figure 12aaii). The negative impact of climate on the maximum LAI of rice is statistically not significant. CO_2 has a significant positive impact on the maximum LAI trend with a trend value of $0.033 \text{ m}^2/\text{m}^2/\text{yr}$ (Figure 12aiii). Nitrogen fertilization has a significant positive impact on the maximum LAI trend, with a value of $0.034 \text{ m}^2/\text{m}^2/\text{yr}$ (Figure 12aiv). Irrigation has the least impact among the drivers investigated in this study, with a trend value of $0.002 \text{ m}^2/\text{m}^2/\text{yr}$ (Figure 12av). Higher CO_2 and nitrogen fertilization individually have a high positive trend, with a low contribution from irrigation.



Comparing positive trends due to CO₂ or nitrogen fertilisation alone (Figure 12a_{iii} and 12a_{iv}) to the overall trend in CTRL simulation (Figure 12a_i) the strong coupling of CN cycle is evident in the rice crop.

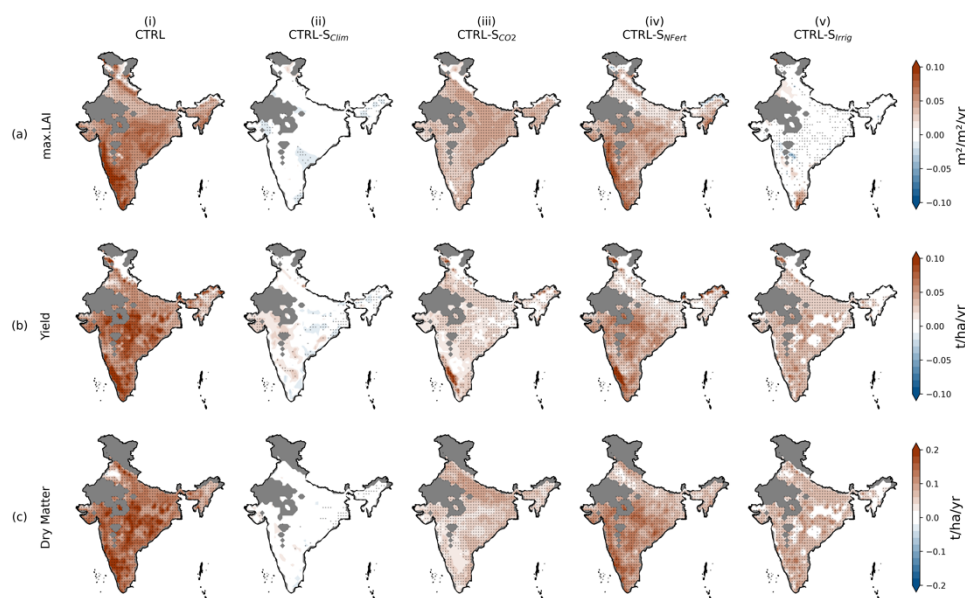


480 **Figure 12: Similar to Figure 8, but for crop physiology in rice.**

The trend in yield for rice simulated by CLM5 from 1970 to 2014 is 58 kg/ha/year (Figure 12b_i). The trend in yield for rice in FAO data is 58 kg/ha/year from 1970 to 2014. The yield simulated by CLM5 in 1970 is 1.3 t/ha, while it is 3.97 t/ha in 2014. Climate has no significant impact on rice yield (Figure 12b_{ii}). CO₂ has a significant positive impact on yield with a Sens slope of 20 kg/ha/year (Figure 12b_{iii}). Nitrogen fertilization has a significant positive impact on yield, with a trend value of 36 kg/ha/year from 1970 to 2014 (Figure 12b_{iv}). Irrigation has a significant positive impact on the yield, with a Sens slope of 26 kg/ha/year during the study period (Figure 12b_v). Nitrogen fertilization has the largest impact on rice yield.

The trend in dry matter of rice from 1970 to 2014 is 126 kg/ha/year (Figure 12c_i). The total dry matter simulated by CLM5 in 1970 for wheat is 4.56 t/ha, while it increased to 9.92 t/ha by 2014. Climate has no significant impact on the total dry matter of rice (Figure 12c_{ii}). CO₂ has a significant positive impact on the total dry matter in rice, with a trend of 53 kg/ha/year (Figure 12c_{iii}). Nitrogen fertilization has a significant impact on the dry matter of rice, with a trend of 88 kg/ha/year (Figure 12c_{iv}). Irrigation has a significant impact on dry matter of rice, with a trend of 57 kg/ha/year (Figure 12c_v). Nitrogen fertilization has the most significant impact on total dry matter accumulated during a growing season in rice.

Figure 13 shows the spatial variation in crop physiology of rice. Higher CO₂ led to increased LAI in rice crops across the rice growing region (Figure 13a_{iii}). However, the impact on yield is not significant in all rice-growing regions (Figure 13b_{ii}). The rice yield has no significant impact due to higher CO₂ in the southern regions. In comparison, the rice yield has a significant positive impact due to higher CO₂ over the IGP region. Human management practices, fertilization, and irrigation have a positive impact on crop phenology across rice-growing regions. The impact on LAI due to irrigation is inconsistent across rice-growing regions (Figure 13a_v).



500 **Figure 13: Spatial trend observed in (a) max. LAI, (b) Yield, and (c) Dry Matter of rice-growing regions in the (i) CTRL simulation. (ii) to (v) shows the impact of each driver. Regions stippled implies the trend is statistically significant at $p < 0.05$.**

3.3.2 Wheat

The trend in maximum LAI during a growing season for spring wheat is $0.027 \text{ m}^2/\text{m}^2/\text{year}$ (Figure 14ai). The maximum LAI in 1970 is $2.62 \text{ m}^2/\text{m}^2$, while in 2014 it is $4.16 \text{ m}^2/\text{m}^2$. Climate has a significant negative impact on the observed maximum LAI trend, with a trend of $-0.015 \text{ m}^2/\text{m}^2/\text{yr}$ (Figure 14aii). CO₂ has a significant positive impact on the observed maximum LAI trend with a trend value of $0.025 \text{ m}^2/\text{m}^2/\text{yr}$ (Figure 14aiii). Nitrogen fertilization has a significant positive impact on the maximum LAI trend, with a value of $0.008 \text{ m}^2/\text{m}^2/\text{yr}$ (Figure 14aiv). Irrigation has the least impact among the drivers investigated in this study, with a trend value of $0.005 \text{ m}^2/\text{m}^2/\text{yr}$ (Figure 14av). CO₂ has the maximum impact on maximum LAI observed during a growing season of wheat crop. Although climate has a large and significant negative impact on wheat maximum LAI during a growing season (Figure 14aii), the combined positive impact of all other factors has led to a high and significant positive impact (Figure 14ai)

The trend in yield for wheat simulated by CLM5 from 1970 to 2014 is $40 \text{ kg}/\text{ha}/\text{year}$ (Figure 14bi). The trend in yield for wheat in FAO data is $46 \text{ kg}/\text{ha}/\text{year}$ from 1970 to 2014. The yield simulated by CLM5 in 1970 is $1.11 \text{ t}/\text{ha}$, while it is $2.71 \text{ t}/\text{ha}$ in 2014. Climate has no significant impact on wheat yield (Figure 14bii). CO₂ has a significant positive impact on yield with a Sens slope of $19 \text{ kg}/\text{ha}/\text{year}$ (Figure 14biii). Nitrogen fertilization has a significant positive impact on yield, with a trend value of $24 \text{ kg}/\text{ha}/\text{year}$ from 1970 to 2014 (Figure 14biv). Irrigation has the most significant impact on the yield of wheat crops, with a Sens slope of $31 \text{ kg}/\text{ha}/\text{year}$ during the study period (Figure 14bv).

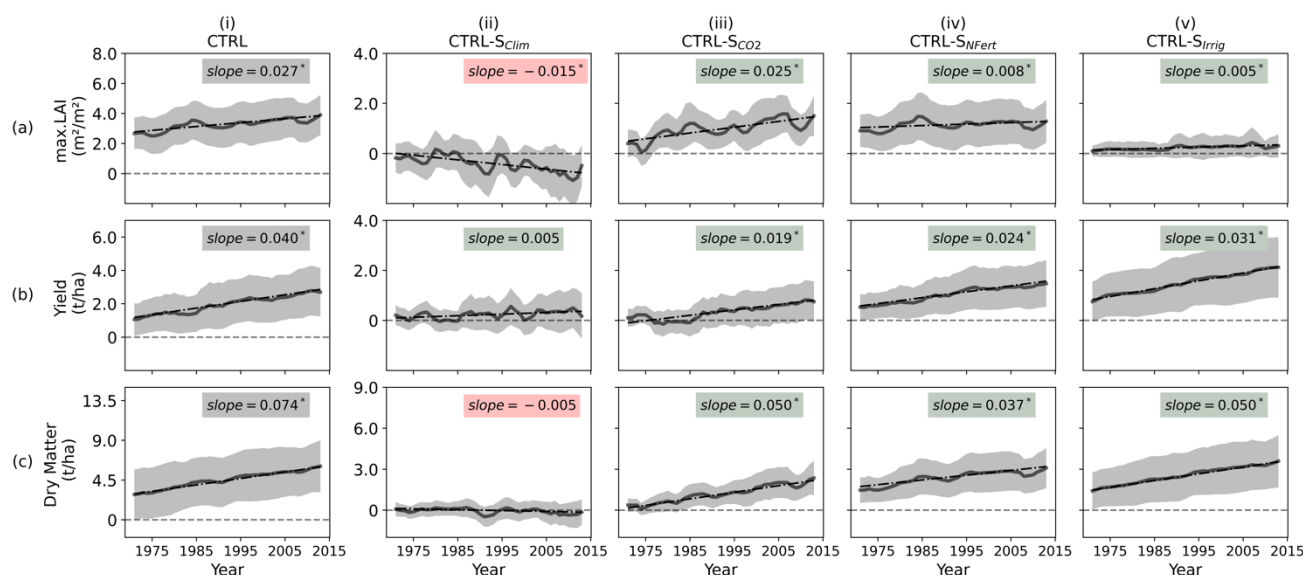


Figure 14: Similar to Figure 8, but for crop phenology in wheat.

520 The trend in dry matter of wheat crops from 1970 to 2014 is 74 kg/ha/year (Figure 14ci). The total dry matter simulated by CLM5 in 1970 for wheat is 2.82 t/ha, while it increased to 6.43 t/ha by 2014. Climate has no significant impact on the total dry matter of wheat crops (Figure 14cii). CO₂ has a significant positive impact on the total dry matter in wheat, with a trend value of 50 kg/ha/year (Figure 14ciii). Nitrogen fertilization has a significant impact on dry matter in wheat, with a trend of 37 kg/ha/year (Figure 14civ). Along with CO₂, irrigation significantly impacts dry matter in wheat, with a trend of 50 kg/ha/year (Figure 14cv). CO₂ has a significant positive impact on LAI in wheat. The agricultural management drivers have a significant positive impact on the yield and dry matter of wheat.

The spatial variation of crop physiology trends and the impact of various drivers over the wheat-growing regions shows that crop physiology has a significant positive trend across the wheat-growing region (Figure S3i), and climate has a significant negative impact on the LAI of wheat across large parts of the wheat-growing regions (Figure S3aii). Climate showed no significant impact on yield across the wheat-growing region (Figure S3bii). CO₂, nitrogen fertilization, and irrigation all have a positive impact on crop phenology of wheat and is statistically significant in large parts of the wheat growing region (Figure S3).

3.4 Trends in water and energy fluxes

3.4.1 Rice

535 The trend in LH during a growing season for rice is 0.103 W/m²/year (Figure 15ai). Figure 15aai to av) show the impact of each of the drivers on the observed positive trend. Climate has no significant impact on the observed LH trend (Figure 15aai). CO₂ has a positive impact on the observed LH trend with a trend value of 0.021 W/m²/yr (Figure 15aaiii). Nitrogen fertilization



has no impact on the LH trend (Figure 15aiv). Irrigation has a statistically significant positive impact among the drivers investigated in this study, with a trend value of $0.010 \text{ W/m}^2/\text{yr}$ (Figure 15av). Climate has the maximum impact on LH but is not significant at $p < .05$, and the impact of irrigation is low but statistically significant.

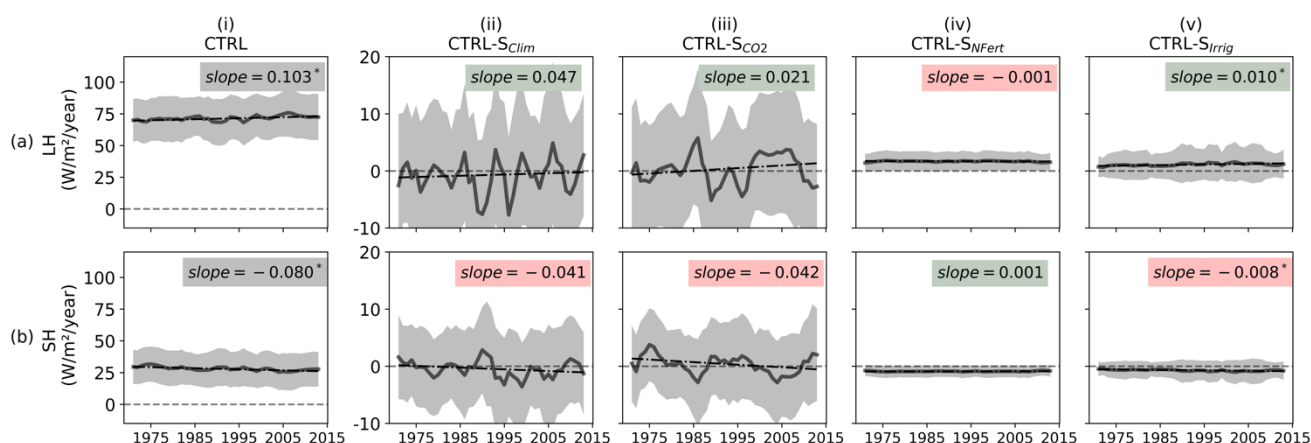


Figure 15: Similar to Figure 8, but for water and energy fluxes in rice-growing regions.

The trend in SH for the rice-growing season simulated by CLM5 from 1970 to 2014 is $-0.080 \text{ W/m}^2/\text{year}$ (Figure 15bi). Climate and CO_2 have no significant impact on SH (Figure 15bii and 15biii). Nitrogen fertilization has no significant impact on SH during the rice-growing season ((Figure 15biv)). Irrigation has the most significant impact on the SH during the rice-growing season, with a Sens slope of $-0.008 \text{ W/m}^2/\text{year}$ during the study period (Figure 15bv).

3.4.2 Wheat

The trend in LH during a growing season for wheat is $0.111 \text{ W/m}^2/\text{year}$ (Figure 16ai). Climate has no significant impact on the observed LH trend (Figure 16aai). CO_2 has no significant impact on the observed LH trend in wheat growing regions (Figure 16aaii). Nitrogen fertilization has no impact on the LH trend (Figure 16aiv). Irrigation has the most significant impact among the drivers investigated in this study, with a trend value of $0.070 \text{ W/m}^2/\text{yr}$ (Figure 16av). Irrigation is the only driver that has a significant impact on the LH trends in the wheat-growing seasons.

The trend in SH of the wheat-growing season from 1970 to 2014 is $-0.047 \text{ W/m}^2/\text{yr}$ (Figure 16bi). Climate, CO_2 , and nitrogen fertilization have no significant impact on the SH trend observed in the control run (Figure 16bii, 16biii, and 16biv). Irrigation has the most significant impact on the SH during the wheat-growing season, with a Sens slope of $-0.045 \text{ W/m}^2/\text{yr}$ during the study period (Figure 16bv).

Irrigation has a statistically significant impact on energy and water fluxes over the wheat-growing regions. The impact of irrigation in rice-growing regions is low. The low impact in rice growing regions might be because of the growing season (kharif season), in which most of the water requirements are met through rainfall and less irrigation water is required.

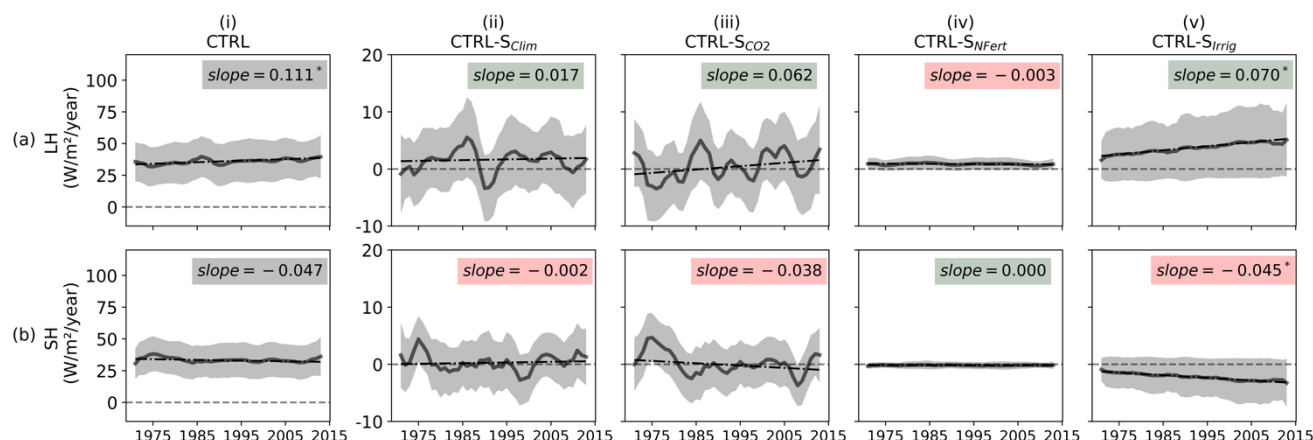


Figure 16: Similar to Figure 8, but for water and energy fluxes in wheat-growing regions.

3.5 Annual yield

The annual country-scale wheat and rice yield simulated by CLM5 in 1970 was 1.11 and 1.3 t/ha, respectively. The wheat and rice yield reported by FAO for the same year is 1.2 and 1.6 t/ha. The rice yield simulated by CLM5 is lower than FAO data in the year 1970. However, for the year 2014 CLM5 simulated 2.71 and 3.63 t/ha for wheat and rice, respectively, while FAO estimates are 3.14 and 3.57 t/ha. CLM5 is simulating annual country scale yield accurately for two major Indian crops, and the CLM5 model can be used for future climate impact studies with high confidence at a regional scale.

The impact of management practices on yield is significant (Figure 17). Irrigation has a significant impact on wheat yield. The average wheat yield simulated in the CTRL experiment over the period 2010-2014 is 2.74 t/ha, while the simulation with no irrigation has an average yield of 0.64 t/ha for the same period. Similarly, the lack of nitrogen fertilization decreased the mean yield during the same period to 1.26 t/ha. In the case of rice crops, fertilization has a more significant impact than irrigation. Therefore, for a wheat crop grown in cold and dry conditions, irrigation is the dominant factor, and for rice grown in warm and wet conditions, nitrogen fertilisation is the dominant management factor.

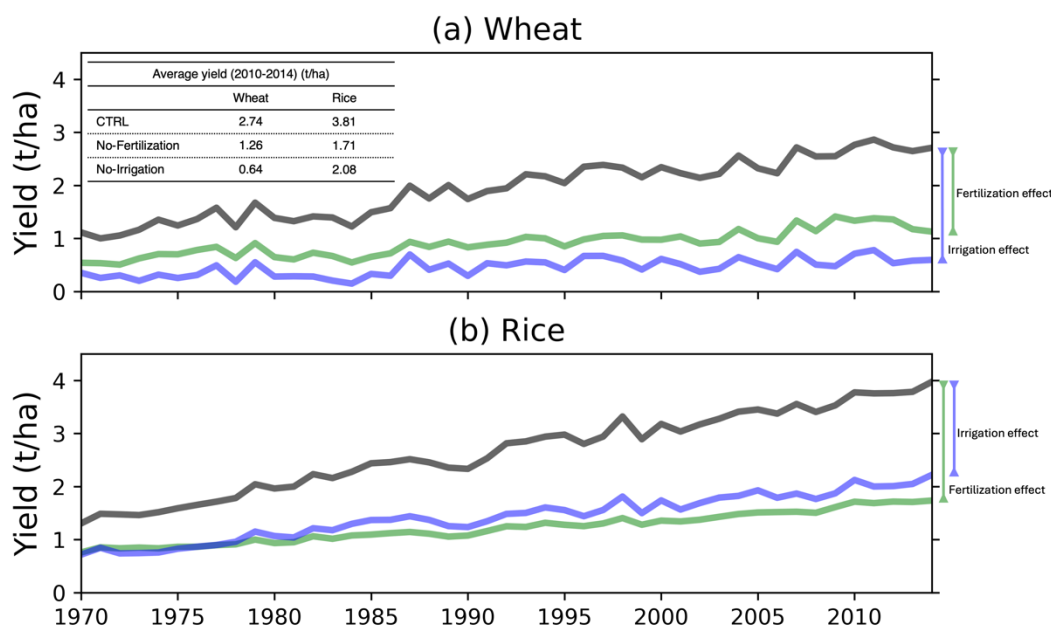


Figure 17: Impact of management drivers on crop yield of (a) wheat and (b) rice

3.6 Comparing seasonal carbon fluxes against global studies

CLM5 simulated cumulative GPP for kharif rice from 2000 to 2014 is 1528.3 ± 561 gC/m². This is comparable to other site scale observations (Table S1). For example, at a site in India (20°27' N, 85°56' E) GPP is 929 and 1221 gC/m² (Bhattacharyya et al., 2014), at a site in the Philippines (14°14' N, 121°26' E) it is 1192 and 1464 gC/m² (Alberto et al., 2009), and Bangladesh (24°73' N, 90°42' E) is 1312 and 1574 gC/m² (Hossen et al., 2011). A site in India (11°00' N, 79°28' E) is 2355 gC/m² and 2598 gC/m² for the three rice crop periods in a year (Oo et al., 2023). All studies mentioned above, except Oo et al. (2023), had two growing seasons: wet and dry. CLM5 simulations also include rainfed and irrigated rice crops, and therefore, the annual simulated GPP is in the same range as all other studies, while it is lower than the GPP estimates by Oo et al. (2023). Bhattacharya et al. (2012) studied the impact of fertilization on carbon fluxes over rice fields. They observed that fertilization usage had increased the GPP by 68.9%. In comparison, our study simulates an increase in GPP by 68.4% to 78.9% from using nitrogen fertilization from 2000 to 2014.

CLM5 simulated cumulative GPP for rabi wheat from 2000 to 2014 is 862.6 ± 438.6 gC/m². This is comparable with site scale observations. For example, rabi wheat cumulative GPP estimates at IARI (28°40' N, 77°12' E) is 949.68 gC/m² (Reddy et al., 2023) and 888 gC/m² (Kumar et al., 2021), at Saharanpur (29° 52' N and 77° 34' E) is 1024 gC/m² (Patel et al., 2021). CLM5 simulates the cumulative GPP reasonably well during the growing season of wheat in Indian conditions (Table S1). The carbon fluxes over a wheat growing season in Germany (50°52' N, 6°26' E) are 1304 and 1067 gC/m² (Schmidt et al., 2012), and in China (32°33' N, 116°47' E), are 987 and 966 gC/m² (Chen et al., 2015). Higher seasonal cumulative fluxes in Germany and China are due to the longer growing seasons observed in these regions .



595 AR/GPP ratio has reduced from 0.62 in the 1970-75 period to 0.46 in 2010-14. During the same period, nitrogen fertilization increased rapidly, leading to lower respiration losses, evident from nitrogen fertilization's impact on autotrophic respiration in section 3.2. CLM5 limits the maintenance respiration if high nitrogen is present in the leaves.

3.7 Comparing water and energy fluxes against global studies

The evapotranspiration simulated by CLM5 during the Kharif season from 2000 to 2014 is 558.82 mm. The observations from
600 a site in India (11°00' N, 79°28' E) during the kharif season are 529 and 392 mm (Oo et al., 2023). The lower evapotranspiration in the second year is due to the lack of data for the last 27 days of the rice growing season (Oo et al., 2023). A study by Hossen et al. (2011) focusing on rice crops in Bangladesh (24°43' N, 90°25' E) reported seasonal evapotranspiration of 370 and 307 mm when measured from transplanting to harvest. The lower evapotranspiration values are due to the consideration of transplanting to harvest instead of sowing to harvest. The CLM5 simulation of seasonal evapotranspiration is comparable to
605 site-scale observations. The evapotranspiration simulated by CLM5 during the Rabi season from 2000 to 2014 is 277.92 mm. Irrigation in the wheat growing season (Rabi season) has a significant impact on evapotranspiration. Since CLM5 is now performing well in estimating the water and energy fluxes and irrigation is having a significant impact, future studies should examine the impact of varying irrigation levels on the land-atmosphere feedback, similar to the study by Mathur and AchutaRao (2020).

610 5 Discussions and Conclusions

The current study aimed to understand the trends in crop physiological parameters and terrestrial fluxes over major Indian agroecosystems spanning 45 years from 1970 to 2014. This study used the best performing CLM5 model from Reddy et al. (2025) to, first, evaluate the performance of CLM5 in simulating crop physiological parameters and various land fluxes (e.g., energy, carbon, and water fluxes) over two major Indian agroecosystems - wheat and rice. Reanalysis data and in-situ
615 observations are used to perform a comprehensive evaluation of the model and investigate the biases. Later, numerical experiments are conducted to investigate the impact of two natural and two agricultural management drivers – atmospheric CO₂, climate, nitrogen fertilization and irrigation.

CLM5 simulated the crop physiology with realistic seasonality and low bias. Although a high bias in yield is observed at site scale, the country scale estimates of crop yield against FAO data highlights that CLM5 captured the annual variability with a
620 low bias (section 3.1.1). Therefore, providing confidence in CLM5 for estimating climate impact on regional crop yields. CLM5 captures the seasonality in carbon fluxes well with a Pearsons correlation of 0.65. Regional scale carbon flux evaluation against the FLUXCOM data reveals that the carbon fluxes simulated during the kharif season (warm and wet conditions) exhibit a larger bias than the fluxes in rabi season (cold and dry conditions) (section 3.1.2). Comparing the water and energy fluxes also reveals a similar trend, where high bias is observed in latent heat fluxes during the warm and wet seasons compared
625 to those in the cold and dry season (section 3.1.3). The contrasting simulation of carbon and energy fluxes in different seasons highlights the need to investigate the stomatal conductance module in CLM5. Sensitivity experiments can be conducted to



understand the role of stomatal conductance in simulating a high bias in carbon, water, and energy fluxes during warm and wet seasons in the Indian region.

The underestimation of GPP and overestimation of TER over the rice-growing regions during the kharif season mainly stems from shortcomings in land management practices for crops. Rice is grown in flooded fields which tend to have lower GPP and TER. CLM5 does not simulate rice in flooded conditions. Additionally, rice is grown multiple times in a year in India, especially in the central and southern regions of India, which is absent in CLM5 mainly due to the lack of crop maps that represent the multiple cropping followed in India. Although a few studies have reported multiple rice cropping maps (Zhao et al., 2024), they are limited to one or two years, and we do not have time varying maps to conduct transient model simulations. It is important that future research focuses on generating multiple-cropping maps for regions like India because rice, for example, grown in multiple seasons has a large impact on the terrestrial fluxes (Oo et al., 2023).

The vegetation physiology and phenology substantially affect the land surface processes and influences the local to global climates through interactions between the land and atmosphere. Although CLM5 has few limitations, it performs well in capturing the seasonal patterns and magnitude of carbon and water fluxes over the Indian agroecosystems. A future study can focus on estimating the terrestrial fluxes in the near future and end century climate in Indian agroecosystems using the reasonably well performing CLM5 model. The climate change impact is necessary to understand because the terrestrial ecosystems are taking up lower carbon in a warming climate (Liu et al., 2024; Ke et al., 2024) and it is essential to identify the tipping points of various ecosystems as these will have drastic impact on the world.

More modeling studies such as the current one are crucial in understanding and reducing the uncertainty in simulated terrestrial fluxes of various ecosystems using limited observation data. Increasingly, studies are identifying lower carbon uptake by terrestrial ecosystems using observations. Models are failing to replicate the same and to worsen the situation models are simulating with large uncertainties (Friedlingstein et al., 2023). Studies such as the current one will help in identifying the regions and processes responsible for model uncertainty. Adaptation of recent developments in terrestrial ecosystem representations in land models such as Eco-Evolutionary Optimality theory (Harrison et al., 2021; Zou et al., 2023) should be investigated and implemented in various land models such as CLM5. The adaptation of new theories might reduce the high biases in water, energy and carbon fluxes observed in different seasons. The shift to new theories is necessary as they use a smaller number of parameters for simulating terrestrial fluxes and are less sensitive to uncertainties in input data (Zou et al., 2023).

Data and code availability: The site-scale data used in the study are available in Varma et al. (2024) (<https://doi.org/10.1594/PANGAEA.964634>). The model output data for various experiments of the study and the observational data are available at <https://doi.org/10.5281/zenodo.15291023>. Python codes used to produce the figures in the manuscript are also available in the Zenodo repository.

Competing interests: The authors declare that they have no conflict of interest.



Acknowledgements: The authors thank the IIT Delhi HPC facility for computational resources. Scientific color maps (Crameri et al., 2018) are used in this study to prevent visual distortion of the data and exclusion of readers with color-vision deficiencies (Crameri et al., 2020).

665 References

- Alberto, M. C. R., Wassmann, R., Hirano, T., Miyata, A., Kumar, A., Padre, A., and Amante, M.: CO₂/heat fluxes in rice fields: Comparative assessment of flooded and non-flooded fields in the Philippines, *Agr. Forest Meteorol.*, 149, 1737–1750, <https://doi.org/10.1016/j.agrformet.2009.06.003>, 2009.
- ASG-2023: Agricultural Statistics at a Glance 2023, Division of Economics, Statistics and Evaluation, Department of Agriculture and Farmers Welfare, Ministry of Agriculture and Farmers Welfare, Government of India, https://desagri.gov.in/wp-content/uploads/2025/01/%E0%A4%95%E0%A5%83%E0%A4%B7%E0%A4%BF%E0%A4%B8%E0%A4%BE%E0%A4%82%E0%A4%96%E0%A5%8D%E0%A4%AF%E0%A4%BF%E0%A4%95%E0%A5%80%E0%A4%8F%E0%A4%95%E0%A4%9D%E0%A4%B2%E0%A4%95-2023_Agricultural-Statistics-at-a-Glance-2023.pdf (last access: April, 2025), 2024.
- 670 Badger, A. M. and Dirmeyer, P. A.: Climate response to Amazon forest replacement by heterogeneous crop cover, *Hydrol. Earth Syst. Sci.*, 19, 4547–4557, <https://doi.org/10.5194/hess-19-4547-2015>, 2015.
- Bhattacharyya P., Neogi S., Roy K. S., Dash P. K., Tripathi R., and Rao K. S.: Net ecosystem CO₂ exchange and carbon cycling in tropical lowland flooded rice ecosystem. *Nutr. Cycl. Agroecosyst.*, 95:133–144, <https://doi.org/10.1007/s10705-013-9553-1>, 2013.
- 680 Boas, T., Bogen, H., Grünwald, T., Heinesch, B., Ryu, D., Schmidt, M., Vereecken, H., Western, A., and Hendricks Franssen, H.-J.: Improving the representation of cropland sites in the Community Land Model (CLM) version 5.0, *Geosci. Model Dev.*, 14, 573–601, <https://doi.org/10.5194/gmd-14-573-2021>, 2021.
- Boas, T., Bogen, H. R., Ryu, D., Vereecken, H., Western, A., and Hendricks Franssen, H.-J.: Seasonal soil moisture and crop yield prediction with fifth-generation seasonal forecasting system (SEAS5) long-range meteorological forecasts in a
- 685 land surface modeling approach, *Hydrol. Earth Syst. Sci.*, 27, 3143–3167, <https://doi.org/10.5194/hess-27-3143-2023>, 2023
- Bonan, G. B. and Doney, S. C.: Climate, ecosystems, and planetary futures: The challenge to predict life in Earth system models, *Science*, 359, eaam8328, <https://doi.org/10.1126/science.aam8328>, 2018.
- Chen, C., Dan, L.I., Zhiqiu, G., Tang, J., Xiaofeng, G., Linlin, W., and Bingcheng, W.: Seasonal and interannual variations of carbon exchange over a rice-wheat rotation system on the north china plain, *Advan. Atmos. Sci.*, 32, 1365–1380, <https://doi.org/10.1007/s00376-015-4253-1>, 2015.
- 690 Chenu, K., Porter, J.R., Martre, P., Basso, B., Chapman, S.C., Ewert, F., Bindi, M. and Asseng, S.: Contribution of crop models to adaptation in wheat, *Trends Plant Sci.*, 22(6), pp.472–490, <https://doi.org/10.1016/j.tplants.2017.02.003>, 2017.
- Cheng, Y., Huang, M., Zhu, B., Bisht, G., Zhou, T., Liu, Y., Song, F., and He, X.: Validation of the Community Land Model Version 5 Over the Contiguous United States (CONUS) Using In-Situ and Remote Sensing Data Sets, *J. Geophys. Res.-Atmos.*, 126, 1–27, <https://doi.org/10.1029/2020JD033539>, 2021.
- Crameri, F.: Scientific color maps, Zenodo, <https://doi.org/10.5281/zenodo.1243862>, 2018.
- Crameri, F., Shephard, G. E., and Heron, P. J.: The misuse of color in science communication, *Nat. Commun.*, 11, 5444, <https://doi.org/10.1038/s41467-020-19160-7>, 2020.
- 700 Collier, N., Hoffman, F. M., Lawrence, D. M., Keppel-Aleks, G., Koven, C. D., Riley, W. J., Mu, M., and Randerson, J. T.: The International Land Model Benchmarking (ILAMB) System: Design, Theory, and Implementation, *J. Adv. Model. Earth Sy.*, 10, 2731–2754, <https://doi.org/10.1029/2018MS001354>, 2018.



- Denager, T., Sonnenborg, T. O., Looms, M. C., Bogen, H., and Jensen, K. H.: Point-scale multi-objective calibration of the Community Land Model (version 5.0) using in situ observations of water and energy fluxes and variables, *Hydrol. Earth Syst. Sci.*, 27, 2827–2845, <https://doi.org/10.5194/hess-27-2827-2023>, 2023.
- FAO: FAOSTAT statistical database: Production, <https://www.fao.org/faostat/en/#data> (last access: 20 October 2024), 2022a.FAO
- Fisher, R. A. and Koven, C. D.: Perspectives on the Future of Land Surface Models and the Challenges of Representing Complex Terrestrial Systems, *J. Adv. Model. Earth Sy.*, 12, e2018MS001453, <https://doi.org/10.1029/2018ms001453>, 2020.
- Friedlingstein, P., O'Sullivan, M., Jones, M. W., Andrew, R. M., Bakker, D. C. E., Hauck, J., Landschützer, P., Le Quéré, C., Luijkx, I. T., Peters, G. P., Peters, W., Pongratz, J., Schwingshackl, C., Sitch, S., Canadell, J. G., Ciais, P., Jackson, R. B., Alin, S. R., Anthoni, P., Barbero, L., Bates, N. R., Becker, M., Bellouin, N., Decharme, B., Bopp, L., Brasika, I. B. M., Cadule, P., Chamberlain, M. A., Chandra, N., Chau, T.-T.-T., Chevallier, F., Chini, L. P., Cronin, M., Dou, X., Enyo, K., Evans, W., Falk, S., Feely, R. A., Feng, L., Ford, D. J., Gasser, T., Ghattas, J., Gkritzalis, T., Grassi, G., Gregor, L., Gruber, N., Gürses, Ö., Harris, I., Hefner, M., Heinke, J., Houghton, R. A., Hurtt, G. C., Iida, Y., Ilyina, T., Jacobson, A. R., Jain, A., Jarníková, T., Jersild, A., Jiang, F., Jin, Z., Joos, F., Kato, E., Keeling, R. F., Kennedy, D., Klein Goldewijk, K., Knauer, J., Korsbakken, J. I., Körtzinger, A., Lan, X., Lefèvre, N., Li, H., Liu, J., Liu, Z., Ma, L., Marland, G., Mayot, N., McGuire, P. C., McKinley, G. A., Meyer, G., Morgan, E. J., Munro, D. R., Nakaoka, S.-I., Niwa, Y., O'Brien, K. M., Olsen, A., Omar, A. M., Ono, T., Paulsen, M., Pierrot, D., Pocock, K., Poulter, B., Powis, C. M., Rehder, G., Resplandy, L., Robertson, E., Rödenbeck, C., Rosan, T. M., Schwinger, J., Séférian, R., Smallman, T. L., Smith, S. M., Sospedra-Alfonso, R., Sun, Q., Sutton, A. J., Sweeney, C., Takao, S., Tans, P. P., Tian, H., Tilbrook, B., Tsujino, H., Tubiello, F., van der Werf, G. R., van Ooijen, E., Wanninkhof, R., Watanabe, M., Wimart-Rousseau, C., Yang, D., Yang, X., Yuan, W., Yue, X., Zaehle, S., Zeng, J., and Zheng, B.: Global Carbon Budget 2023, *Earth Syst. Sci. Data*, 15, 5301–5369, <https://doi.org/10.5194/essd-15-5301-2023>, 2023.
- Gahlot, S., Lin, T.-S., Jain, A. K., Baidya Roy, S., Sehgal, V. K., and Dhakar, R.: Impact of environmental changes and land management practices on wheat production in India, *Earth Syst. Dynam.*, 11, 641–652, <https://doi.org/10.5194/esd-11-641-2020>, 2020.
- Green, J. K., Seneviratne, S. I., Berg, A. M., Findell, K. L., Hagemann, S., Lawrence, D. M., and Gentile, P.: Large influence of soil moisture on long-term terrestrial carbon uptake, *Nature*, 565, 476–479, <https://doi.org/10.1038/s41586-018-0848-x>, 2019.
- Harrison, S. P., Cramer, W., Franklin, O., Prentice, I. C., Wang, H., Brännström, Å., de Boer, H., Dieckmann, U., Joshi, J., Keenan, T. F., Lavergne, A., Manzoni, S., Mengoli, G., Morfopoulos, C., Peñuelas, J., Pietsch, S., Rebel, K. T., Ryu, Y., Smith, N. G., Stocker, B. D., and Wright, I. J.: Eco-evolutionary optimality as a means to improve vegetation and land-surface models, *New Phytol.*, 231, 2125–2141, <https://doi.org/10.1111/nph.17558>, 2021.
- Hossen, M. S., Mano, M., Miyata, A., Baten, M. A., and Hiyama, T.: Seasonality of ecosystem respiration in a double-cropping paddy field in Bangladesh, *Biogeosciences Discuss.*, 8, 8693–8721, <https://doi.org/10.5194/bgd-8-8693-2011>, 2011.
- Hussain, M. M., and Mahmud, I.: pyMannKendall: a python package for non-parametric Mann Kendall family of trend tests, *J. Open Source Softw.*, 4(39), 1556, <https://doi.org/10.21105/joss.01556>, 2019.
- Ingwersen, J., Högy, P., Witzmann, H. D., Warrach-Sagi, K., and Streck, T.: Coupling the land surface model Noah-MP with the generic crop growth model Gecros: Model description, calibration and validation, *Agr. Forest Meteorol.*, 262, 322–339, <https://doi.org/10.1016/j.agrformet.2018.06.023>, 2018.
- Jung, M., Koirala, S., Weber, U., Ichii, K., Gans, F., Camps-Valls, G., Papale, D., Schwalm, C., Tramontana, G., and Reichstein, M.: The FLUXCOM ensemble of global land-atmosphere energy fluxes, *Sci. Data.*, 6, <https://doi.org/10.1038/s41597-019-0076-8>, 2019.



- Konecky, B.L., McKay, N.P., Falster, G.M., Stevenson, S.L., Fischer, M.J., Atwood, A.R., Thompson, D.M., Jones, M.D., Tyler, J.J., DeLong, K.L. and Martrat, B.: Globally coherent water cycle response to temperature change during the past two millennia. *Nat. Geosci.*, 16(11), pp.997-1004, <https://doi.org/10.1038/s41561-023-01291-3>, 2023.
- 750 Ke, P., Ciais, P., Sitch, S., Li, W., Bastos, A., Liu, Z., Xu, Y., Gui, X., Bian, J., Goll, D. S., Xi, Y., Li, W., O'Sullivan, M., de Souza, J. G., Friedlingstein, P., Chevallier, F.: Low latency carbon budget analysis reveals a large decline of the land carbon sink in 2023, *Atmospheric and Oceanic Physics*, <https://doi.org/10.48550/arXiv.2407.12447>, 2024.
- Koven, C. D., Hugelius, G., Lawrence, D. M., and Wieder, W. R.: Higher climatological temperature sensitivity of soil carbon in cold than warm climates, *Nat. Clim. Change*, 7, 817, <https://doi.org/10.1038/nclimate3421>, 2017.
- 755 Kumar, A., Bhatia, A., Sehgal, V. K., Tomer, R., Jain, N., and Pathak, H.: Net Ecosystem Exchange of Carbon Dioxide in Rice-Spring Wheat System of Northwestern Indo-Gangetic Plains, *Land*, 10, 701, <https://doi.org/10.3390/land10070701>, 2021.
- Lal, M.; Singh, K.K.; Rathore, L.S.; Srinivasan, G.; Saseendram, S.A. Vulnerability of rice and wheat yields in NW India to future changes in climate. *Agric. For. Meteorol.*, 89, 101–114, [https://doi.org/10.1016/S0168-1923\(97\)00064-6](https://doi.org/10.1016/S0168-1923(97)00064-6), 1998.
- 760 Lawrence, D. M., Fisher, R., Koven, C., Oleson, K., Svenson, S., Vertenstein, M. (coordinating lead authors), Andre, B., Bonan, G., Ghimire, B., van Kampenhout, L., Kennedy, D., Kluzek, E., Knox, R., Lawrence, P., Li, F., Li, H., Lombardozzi, D., Lu, Y., Perket, J., Riley, W., Sacks, W., Shi, M., Wieder, W., Xu, C. (lead authors), Ali, A., Badger, A., Bisht, G., Broxton, P., Brunke, M., Buzan, J., Clark, M., Craig, T., Dahlin, K., Drewniak, B., Emmons, L., Fisher, J., Flanner, M., Gentine, P., Lenaerts, J., Levis, S., Leung, L. R., Lipscomb, W., Pelletier, J., Ricciuto, D., M., Sanderson, B., Shuman, J., Slater, A., Subin, Z., Tang, J., Tawfik, A., Thomas, Q., Tilmes, S., Vitt, F., and Zeng, X.: Technical Description of version 5.0 of the Community Land Model (CLM), Natl. Cent. Atmospheric Res. (NCAR), available at http://www.cesm.ucar.edu/models/cesm2/land/CLM50_Tech_Note.pdf (last access: 08 July 2024), 2018.
- 765 Lawrence, P., Lawrence, D. M., Hurtt, G. C., and Calvin, K. V.: Advancing our understanding of the impacts of historic and projected land use in the Earth System: The Land Use Model Intercomparison Project (LUMIP), AGU Fall Meeting 2019, San Francisco, USA, 9–13 December 2019, abstract: GC23B-01, 2019.
- 770 Lawrence, P. J. and Chase, T. N.: Investigating the climate impacts of global land cover change in the community climate system model, *International J. Climatol.*, 30, 2066–2087, <https://doi.org/10.1002/joc.2061>, 2010.
- Lei, H., Huang, M., Leung, L. R., Yang, D., Shi, X., Mao, J., Hayes, D. J., Schwalm, C. R., Wei, Y., and Liu, S.: Sensitivity of global terrestrial gross primary production to hydrologic states simulated by the Community Land Model using two runoff parameterizations, *Journal of Advances in Modeling Earth Systems*, 6, 658–679, <https://doi.org/10.1002/2013MS000252>, 2014.
- 775 Levis, S., Badger, A., Drewniak, B., Nevison, C. and Ren, X.: CLMcrop yields and water requirements: avoided impacts by choosing RCP 4.5 over 8.5, *Clim. Change*, 146, pp.501-515., <https://doi.org/10.1007/s10584-016-1654-9>, 2018.
- Li, H.-Y., Leung, L. R., Getirana, A., Huang, M., Wu, H., Xu, Y., Guo, J., and Voisin, N.: Evaluating Global Streamflow Simulations by a Physically Based Routing Model Coupled with the Community Land Model, *J. Hydrometeorol.*, 16, 948–971, <https://doi.org/10.1175/JHM-D-14-0079.1>, 2015.
- 780 Liu, J., Baker, D., Basu, S., Bowman, K., Byrne, B., Chevallier, F., He, W., Jiang, F., Johnson, M.S., Kubar, T.L. and Li, X.: The reduced net carbon uptake over Northern Hemisphere land causes the close-to-normal CO₂ growth rate in 2021 La Niña. *Science Advances*, 10(23), p.ead12201, 2024.
- 785 Liu, W., Yang, H., Folberth, C., Wang, X., Luo, Q., and Schulin, R.: Global investigation of impacts of PET methods on simulating crop-water relations for maize, *Agr. Forest Meteorol.*, 221, 164–175, <https://doi.org/10.1016/j.agrformet.2016.02.017>, 2016a.
- Lokupitiya, E., Denning, A. S., Schaefer, K., Ricciuto, D., Anderson, R., Arain, M. A., Baker, I., Barr, A. G., Chen, G., Chen, J. M., Ciais, P., Cook, D. R., Dietze, M. C., El Maayar, M., Fischer, M., Grant, R., Hollinger, D., Izaurrealde, C., Jain, A., Kucharik, C. J., Li, Z., Liu, S., Li, L., Matamala, R., Peylin, P., Price, D., Running, S. W., Sahoo, A., Sprintsin,
- 790



- M., Suyker, A.E., Tian, H., Tonitto, C., Torn, M. S., Verbeeck, H., Verma, S. B., and Xue, Y.: Carbon and energy fluxes in cropland ecosystems: a model-data comparison, *Biogeochemistry*, 129, 53–76, <https://doi.org/10.1007/s10533-016-0219-3>, 2016.
- 795 Lokupitiya, E., Denning, S., Paustian, K., Baker, I., Schaefer, K., Verma, S., Meyers, T., Bernacchi, C. J., Suyker, A., and Fischer, M.: Incorporation of crop phenology in Simple Biosphere Model (SiBcrop) to improve land-atmosphere carbon exchanges from croplands, *Biogeosciences*, 6, 969–986, <https://doi.org/10.5194/bg-6-969-2009>, 2009.
- Lombardozzi, D. L., Lu, Y., Lawrence, P. J., Lawrence, D. M., Swenson, S., Oleson, K. W., Wieder, W. R., and Ainsworth, E. A.: Simulating Agriculture in the Community Land Model Version 5, *J. Geophys. Res.-Biogeo.*, 125, e2019JG005529, <https://doi.org/10.1029/2019JG005529>, 2020.
- 800 Migliavacca, M., Musavi, T., Mahecha, M. D., Nelson, J. A., Knauer, J., Baldocchi, D. D., Perez-Priego, O., Christiansen, R., Peters, J., Anderson, K., Bahn, M., Black, T. A., Blanken, P. D., Bonal, D., Buchmann, N., Caldararu, S., Carrara, A., Carvalhais, N., Cescatti, A., Chen, J., Cleverly, J., Cremonese, E., Desai, A. R., El-Madany, T., Farella, M. M., Fernández-Martínez, M., Filippa, G., Forkel, M., Galvagno, M., Gomasasca, U., Gough, C., Göckede, M., Ibrom, A., Ikawa, H., Janssens, I., Jung, M., Kattge, J., Keenan, T., Knohl, A., Kobayashi, H., Kraemer, G., Law, B. E., Liddell, M., 805 Ma, X., Mammarella, I., Martini, D., Macfarlane, C., Matteucci, G., Montagnani, L., Pabon-Moreno, D., Panigada, C., Papale, D., Pendall, E., Penuelas, J., Phillips, R. P., Reich, P. B., Rossini, M., Rotenberg, E., Scott, R., Stahl, C., Weber, U., Wohlfahrt, G., Wolf, S., Wright, I., Yakir, D., Zaehle, S., and Reichstein, M.: The three major axes of terrestrial ecosystem function, *Nature*, 598, 468–472, <https://doi.org/10.1038/s41586-021-03939-9>, 2021.
- Mahowald, N., Lindsey, K., Munoz, E., Doney, S. C., Lawrence, P. J., Schlunegger, S., Ward, D., Lawrence, D. M., and 810 Hoffman, F.: Interactions between land use change and carbon cycle feedbacks, *Global Biogeochem. Cy.*, 31-1, 96-113, <https://doi.org/10.1002/2016GB005374>, 2016.
- Mathur, R. and AchutaRao, K.: A modelling exploration of the sensitivity of the India's climate to irrigation, *Clim. Dynam.*, 54, 1851–1872, <https://doi.org/10.1007/s00382-019-05090-8>, 2019.
- McGuire, A. D., Lawrence, D. M., Koven, C., Clein, J. S., Burke, E., Chen, G., Jafarov, E., MacDougall, A. H., Marchenko, 815 S., Nicolsky, D., Peng, S., Rinke, A., Ciais, P., Gouttevin, I., Hayes, D. J., Ji, D., Krinner, G., Moore, J. C., Romanovsky, V., Schädel, C., Schaefer, K., Schuur, E. A. G., and Zhuang, Q.: The Dependence of the Evolution of Carbon Dynamics in the Northern Permafrost Region on the Trajectory of Climate Change, *P. Natl. Acad. Sci. USA*, 115, 3882–3887, <https://doi.org/10.1073/pnas.1719903115>, 2018.
- Niu, Z., He, H., Yu, P., Sitch, S., Zhao, Y., Wang, Y., Jain, A.K., Vuichard, N. and Si, B.: Climate Change and CO2 820 Fertilization Have Played Important Roles in the Recent Decadal Vegetation Greening Trend on the Chinese Loess Plateau, *Remote Sens.*, 15(5), p.1233, <https://doi.org/10.3390/rs15051233>, 2023.
- Oo, A. Z., Yamamoto, A., Ono, K., Umamageswari, C., Mano, M., Vanitha, K., Elayakumar, P., Matsuura, S., Bama, K. S., Raju, M. and Inubushi, K.: Ecosystem carbon dioxide exchange and water use efficiency in a triple-cropping rice paddy in Southern India: A two-year field observation, *Sci. Total Environ.*, 854, p.158541, 825 <https://doi.org/10.1016/j.scitotenv.2022.158541>, 2023.
- Özdoğan, M.: Exploring the potential contribution of irrigation to global agricultural primary productivity, *Global Biogeochem. Cy.*, 25, GB3016, <https://doi.org/10.1029/2009GB003720>, 2011.
- Patel, N. R., Dadhwal, V. K., and Saha, S. K.: Measurement and Scaling of Carbon Dioxide (CO2) Exchanges in Wheat Using Flux-Tower and Remote Sensing, *J. Indian. Soc. Remote.*, 39, 383–391, <https://doi.org/10.1007/s12524-011-0107-1>, 2011. 830
- Patel, N. R., Pokhariyal, S., Chauhan, P., and Dadhwal, V. K.: Dynamics of CO2 fluxes and controlling environmental factors in sugarcane (C4)–wheat (C3) ecosystem of dry sub-humid region in India, *Int. J. Biometeorol.*, 65, 1069–1084, <https://doi.org/10.1007/s00484-021-02088-y>, 2021.



- Piao, S., Wang, X., Park, T., Chen, C., Lian, X., He, Y., Bjerke, J. W., Chen, A., Ciais, P., Tommervik, H., Nemani, R. R.,
835 and Myrneni, R. B.: Characteristics, drivers and feedbacks of global greening, *Nat. Rev. Earth Env.*, 1, 14–27,
<https://doi.org/10.1038/s43017-019-0001-x>, 2020.
- PlotDigitizer, version 3.1.6, <https://plotdigitizer.com> (last access: April 2025), 2025.
- Portmann, F. T., Siebert, S., and Döll, P.: Mirca2000 – global monthly irrigated and rainfed crop areas around the year
2000: A new high-resolution data set for agricultural and hydrological modelling, *Global Biogeochem. Cy.*, 24(1), GB1011,
840 [doi:10.1029/2008GB003435](https://doi.org/10.1029/2008GB003435), 2010.
- Raczka, B., Hoar, T. J., Duarte, H. F., Fox, A. M., Anderson, J. L., Bowling, D. R., and Lin, J. C.: Improving CLM5.0
biomass and carbon exchange across the Western United States using a data assimilation system, *J. Adv. Model. Earth
Sy.*, 13, e2020MS002421, <https://doi.org/10.1029/2020MS002421>, 2021.
- Reddy, K. N., Baidya Roy, S., Rabin, S. S., Lombardozzi, D. L., Varma, G. V., Biswas, R., and Naik, D. C.: Improving the
845 representation of major Indian crops in the Community Land Model version 5.0 (CLM5) using site-scale crop data,
Geosci. Model Dev., 18, 763–785, <https://doi.org/10.5194/gmd-18-763-2025>, 2025.
- Reddy, K. N., Gahlot, S., Baidya Roy, S., Varma, G. V., Sehgal, V. K., and Vangala, G.: Carbon fluxes in spring wheat
agroecosystem in India, *Earth Syst. Dynam.*, 14, 915–930, <https://doi.org/10.5194/esd-14-915-2023>, 2023.
- Saito, M., Miyata, A., Nagai, H. and Yamada, T.: Seasonal variation of carbon dioxide exchange in rice paddy field in Japan.
850 *Agric. For. Meteorol.*, 135(1-4), pp.93-109, <https://doi.org/10.1016/j.agrformet.2005.10.007>, 2005.
- Schmidt, M., Reichenau, T.G., Fiener, P. and Schneider, K.: The carbon budget of a winter wheat field: An eddy covariance
analysis of seasonal and inter-annual variability, *Agric. For. Meteorol.*, 165, pp.114-126,
<https://doi.org/10.1016/j.agrformet.2012.05.012>, 2012.
- Seo, H. and Kim, Y.: Forcing the Global Fire Emissions Database burned-area dataset into the Community Land Model
855 version 5.0: impacts on carbon and water fluxes at high latitudes, *Geosci. Model Dev.*, 16, 4699–4713,
<https://doi.org/10.5194/gmd-16-4699-2023>, 2023.
- Song, J., Miller, G. R., Cahill, A. T., Aparecido, L. M. T., and Moore, G. W.: Modeling land surface processes over a
mountainous rainforest in Costa Rica using CLM4.5 and CLM5, *Geosci. Model Dev.*, 13, 5147–5173,
<https://doi.org/10.5194/gmd-13-5147-2020>, 2020.
- 860 Varma, G. V., Reddy, K. N., Baidya Roy, S., Yadav, R., Vangala, G., and Biswas, R.: Indian cereal crops (wheat and rice)
phenology and agricultural management data across Indian croplands from 1960s to 2020. PANGAEA,
<https://doi.pangaea.de/10.1594/PANGAEA.964634>, 2024. [dataset]
- Wagle, P., Gowda, P.H., Northup, B.K., Neel, J.P., Starks, P.J., Turner, K.E., Moriasi, D.N., Xiao, X. and Steiner, J.L.:
Carbon dioxide and water vapor fluxes of multi-purpose winter wheat production systems in the US Southern Great
865 Plains. *Agric. For. Meteorol.*, 310, p.108631, , 2021.
- Wang, K. and Dickinson, R. E.: A review of global terrestrial evapotranspiration: Observation, modeling, climatology, and
climatic variability, *Rev. Geophys.*, 50, RG2005, <https://doi.org/10.1029/2011RG000373>, 2012.
- Yin, D., Yan, J., Li, F., Song, T.: Evaluation of global gridded crop models in simulating sugarcane yield in China, *Atmos.
Ocean. Sci. Lett.*, 16 (2), 100329, <https://doi.org/10.1016/j.aosl.2023.100329>, 2023.
- 870 Yu, G.R., Chen, Z. and Wang, Y. P.: Carbon, water and energy fluxes of terrestrial ecosystems in China, *Agric. For.
Meteorol.*, p.109890, <https://doi.org/10.1016/j.agrformet.2024.109890>, 2024.
- Zanaga, D., Van De Kerchove, R., Daems, D., De Keersmaecker, W., Brockmann, C., Kirches, G., Wevers, J., Cartus, O.,
Santoro, M., Fritz, S., Lesiv, M., Herold, M., Tsendbazar, N.-E., Xu, P., Ramoino, F., and Arino, O.: ESA WorldCover
10 m 2021 v200, Zenodo, <https://doi.org/10.5281/zenodo.7254221>, 2022. [dataset]
- 875 Zhao, Z., Dong, J., Zhang, G., Yang, J., Liu, R., Wu, B. and Xiao, X.: Improved phenology-based rice mapping algorithm by
integrating optical and radar data, *Remote Sens. Environ.*, 315, p.114460, <https://doi.org/10.1016/j.rse.2024.114460>,
2024.



- 880 Zhu, Z. C., Piao, S. L., Myneni, R. B., Huang, M. T., Zeng, Z. Z., Canadell, J. G., Ciais, P., Sitch, S., Friedlingstein, P.,
Arneeth, A., Cao, C. X., Cheng, L., Kato, E., Koven, C., Li, Y., Lian, X., Liu, Y. W., Liu, R. G., Mao, J. F., Pan, Y. Z.,
Peng, S. S., Penuelas, J., Poulter, B., Pugh, T. A. M., Stocker, B. D., Viovy, N., Wang, X. H., Wang, Y. P., Xiao, Z. Q.,
Yang, H., Zaehle, S., and Zeng, N.: Greening of the Earth and its drivers, *Nat. Clim. Change*, 6, 791–795,
<https://doi.org/10.1038/nclimate3004>, 2016.
- 885 Zou, M., Yang, K., Lu, H., Ren, Y., Sun, J., Wang, H., Tan, S. and Zhao, L.: Integrating eco-evolutionary optimality
principle and land processes for evapotranspiration estimation, *J. Hydrol.*, 616, p.128855,
<https://doi.org/10.1016/j.jhydrol.2022.128855>, 2023.